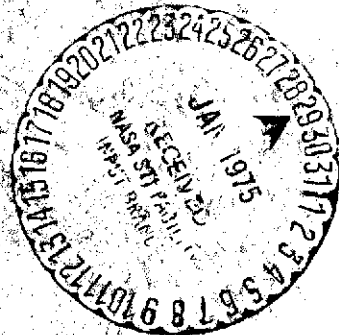


(NASA-CR-120581) REDSHIFT ANTENNA PROJECT N75-14965  
Final Technical Report (Ball Bros. Research  
Corp.) 44 p HC \$3.75 CSCL 09E  
Unclas  
G3/33 08054

# BALL BROTHERS

## RESEARCH CORPORATION





FINAL TECHNICAL REPORT  
For The  
REDSHIFT ANTENNA PROJECT

Project 3260

Contract NAS8-29504  
DRL No. 424, Line Item 2

20 November 1974

Submitted To  
NASA/MSFC

BALL BROTHERS RESEARCH CORPORATION  
Boulder, Colorado



## Table of Contents

<u>Section</u>		<u>Page</u>
A	General Discussion of Antenna Design	2
B	Phase/Temperature Measurements and Analysis	11
C	Temperature Survivability Test	17
D	Conclusions	20



## A. General Discussion of Antenna Design

The program was initiated with the layout of the center frequency 2203.1 MHz antenna. The 4 to 1 taped layout was photograph reduced and a single antenna section (half an antenna) was etched. Initial impedance and frequency mismatches were corrected, first by adding copper tape to the transform lines and trimming the microstrip patches. The artwork was subsequently revised and a complete 2203.1 antenna was etched. Impedance plots of each of the two halves are shown in Figs. 1 and 2. The VSWR of the assembled antenna was good as shown in Fig. 3.

The antenna was mounted on the ground plane mock-up used during the proposal and a 2 dB  $\theta = 90^\circ$  roll pattern was obtained (Fig. 4). Additional effort was required to smooth out the bulges at section joints and center feed points such that the required 3 dB variation at the other aspect angles could be obtained. An aspect pattern of this initial antenna (Fig. 5) indicated that the gains would be acceptable.

Using the 2203.1 MHz layout as a reference, initial layouts were made for the remaining two frequencies 2117.7 and 2299.7 MHz, and single sections fabricated. After encouraging VSWR results at 2117.7 and 2299.7 MHz were obtained, the artwork for the three frequencies were combined into a single antenna system. Several configurations were tested to obtain the best combination of gain, phase and isolation performance. The configuration shown in Fig. 6 was selected. BBRC drawing 46296 defines this configuration and its associated interface requirements in detail.

### IMPEDANCE OR ADMITTANCE COORDINATES

3-26-1

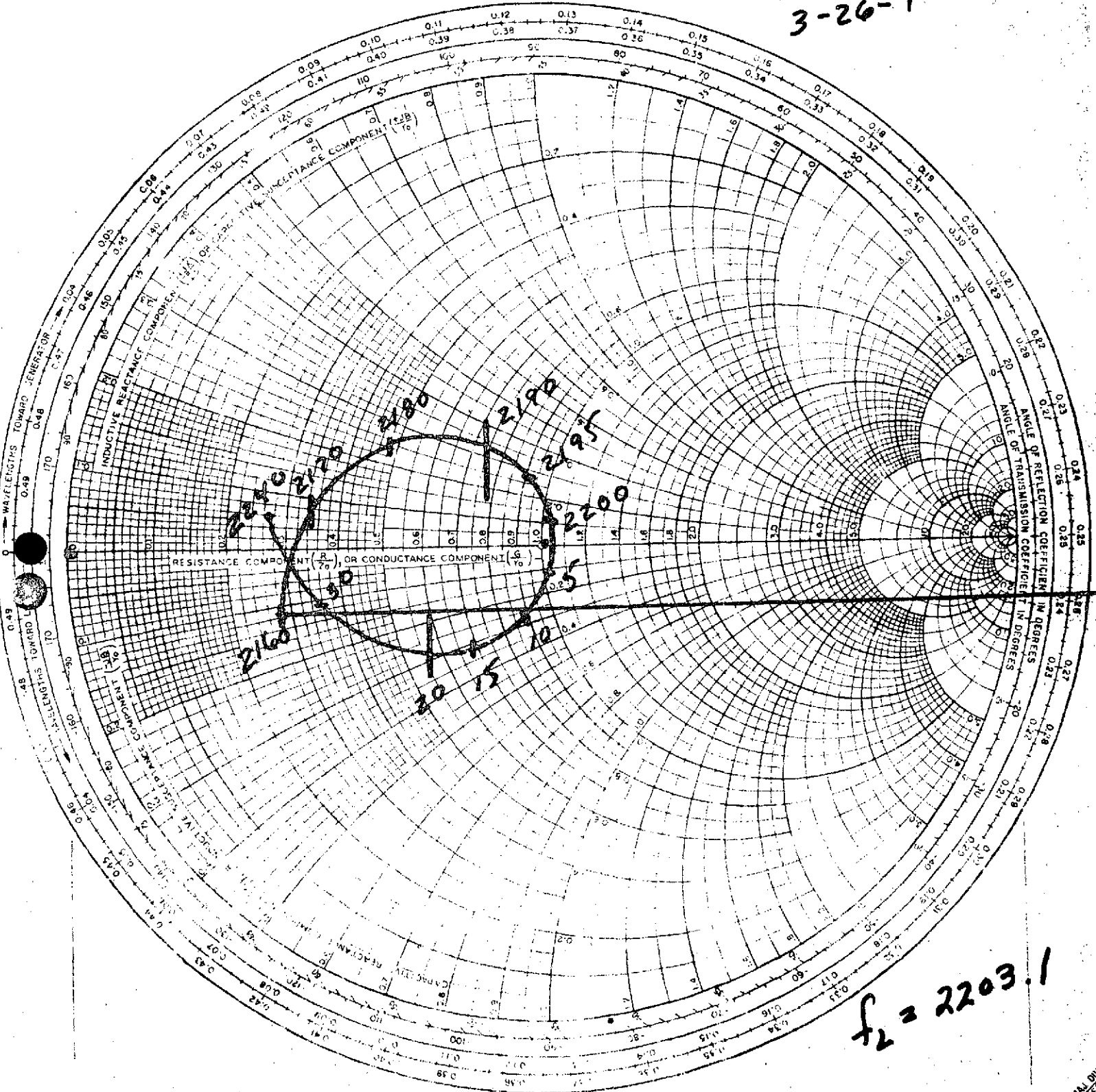
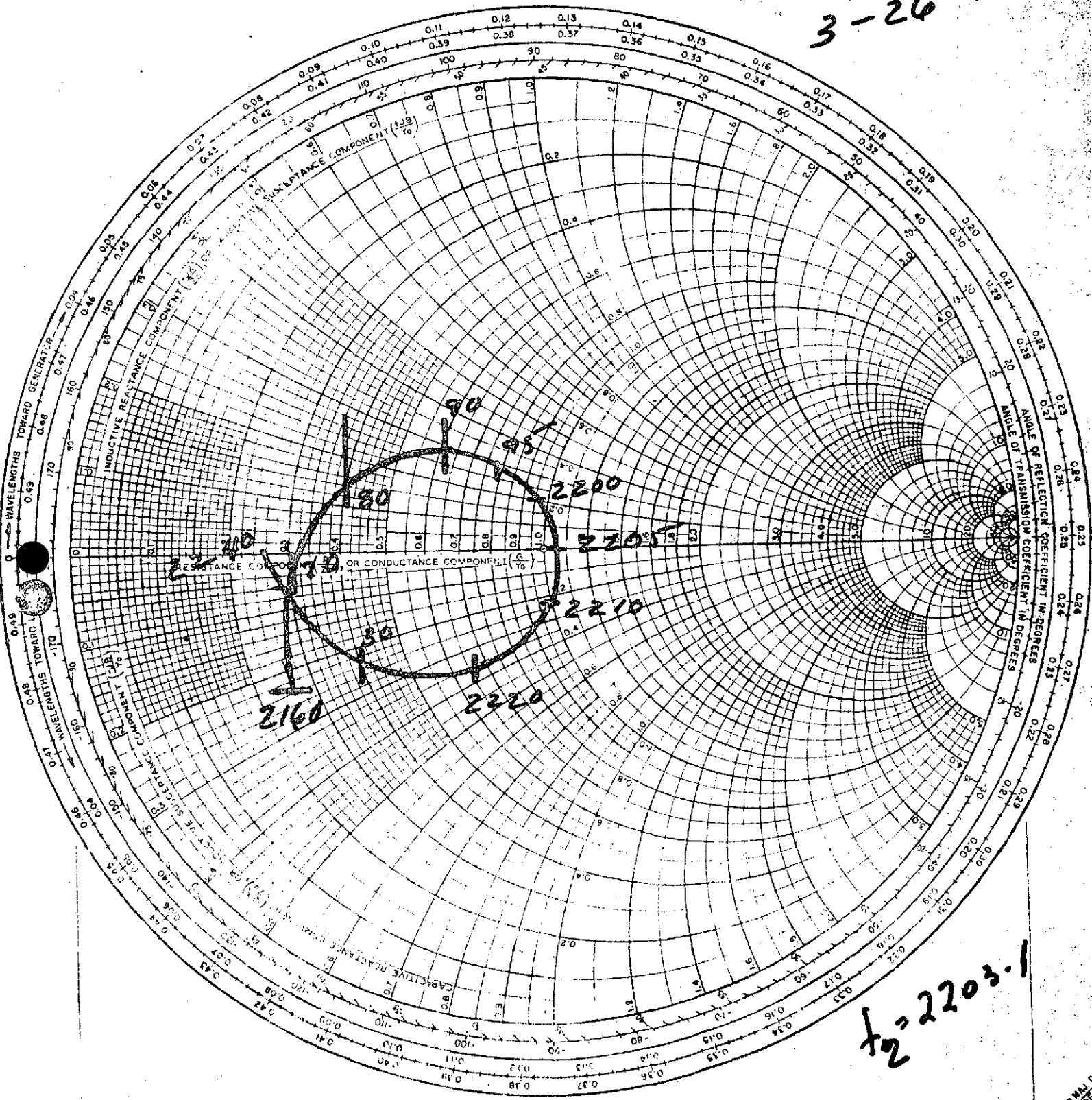


Fig. 1 Impedance Plot of One-Half Initial 2203.1 Antenna

IMPEDANCE OR ADMITTANCE COORDINATES

3-26-2



$\Gamma_{2} = 2203.1$

RADIALLY SCALED PARAMETERS

TOWARD LOAD

TOWARD GENERATOR

Fig. 2 Impedance Plot of Second Half of Initial 2203.1 Antenna

Fig. 3 VSWR of Initial 2203.1 Antenna System

*Red Shift System*

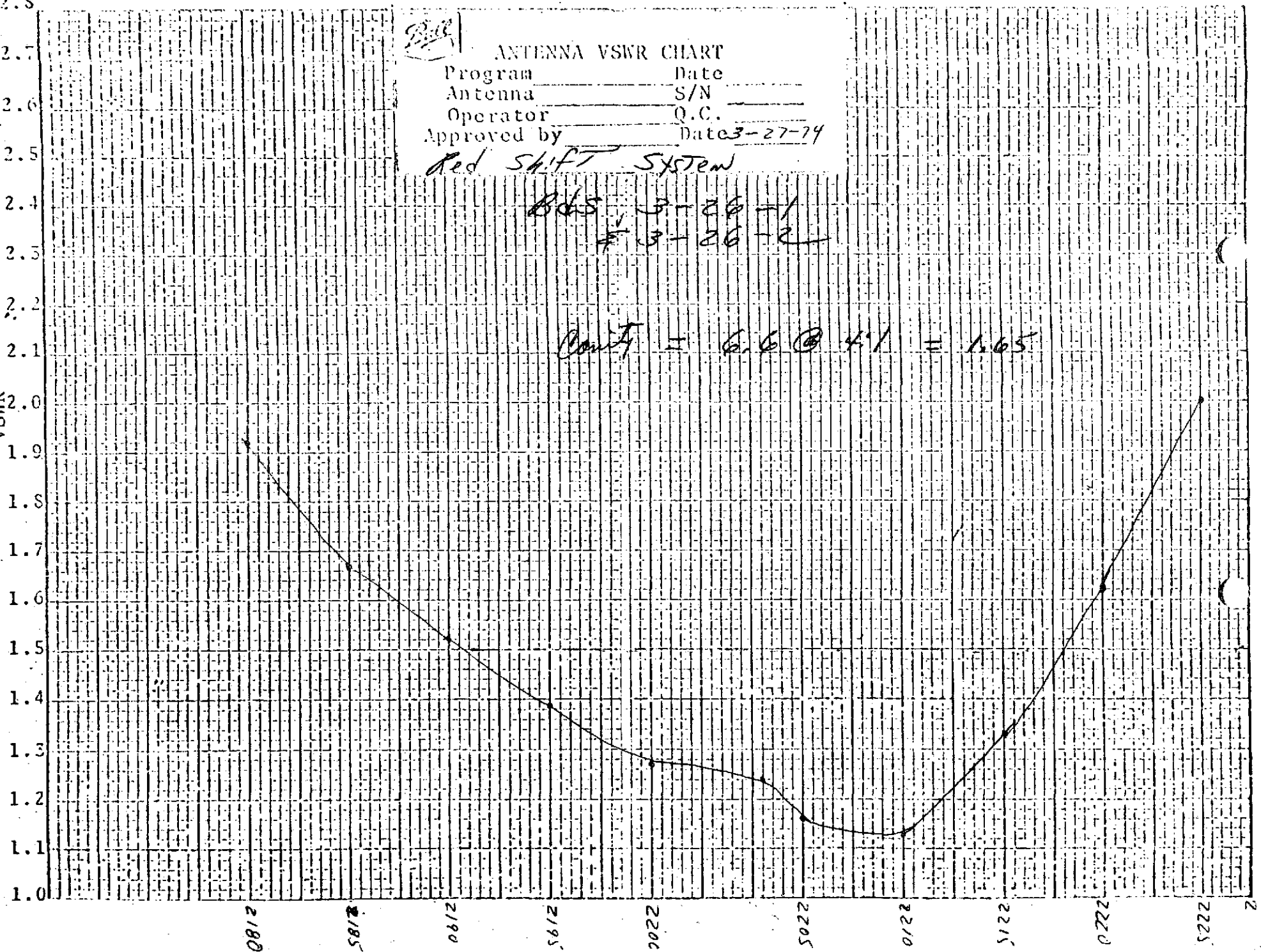
### ANTENNA VSWR CHART

Program \_\_\_\_\_ Date \_\_\_\_\_  
 Antenna \_\_\_\_\_ S/N \_\_\_\_\_  
 Operator \_\_\_\_\_ Q.C. \_\_\_\_\_  
 Approved by \_\_\_\_\_ Date 3-27-74

*Red Shift System*

Obs 3-26-1  
 # 3-26-2

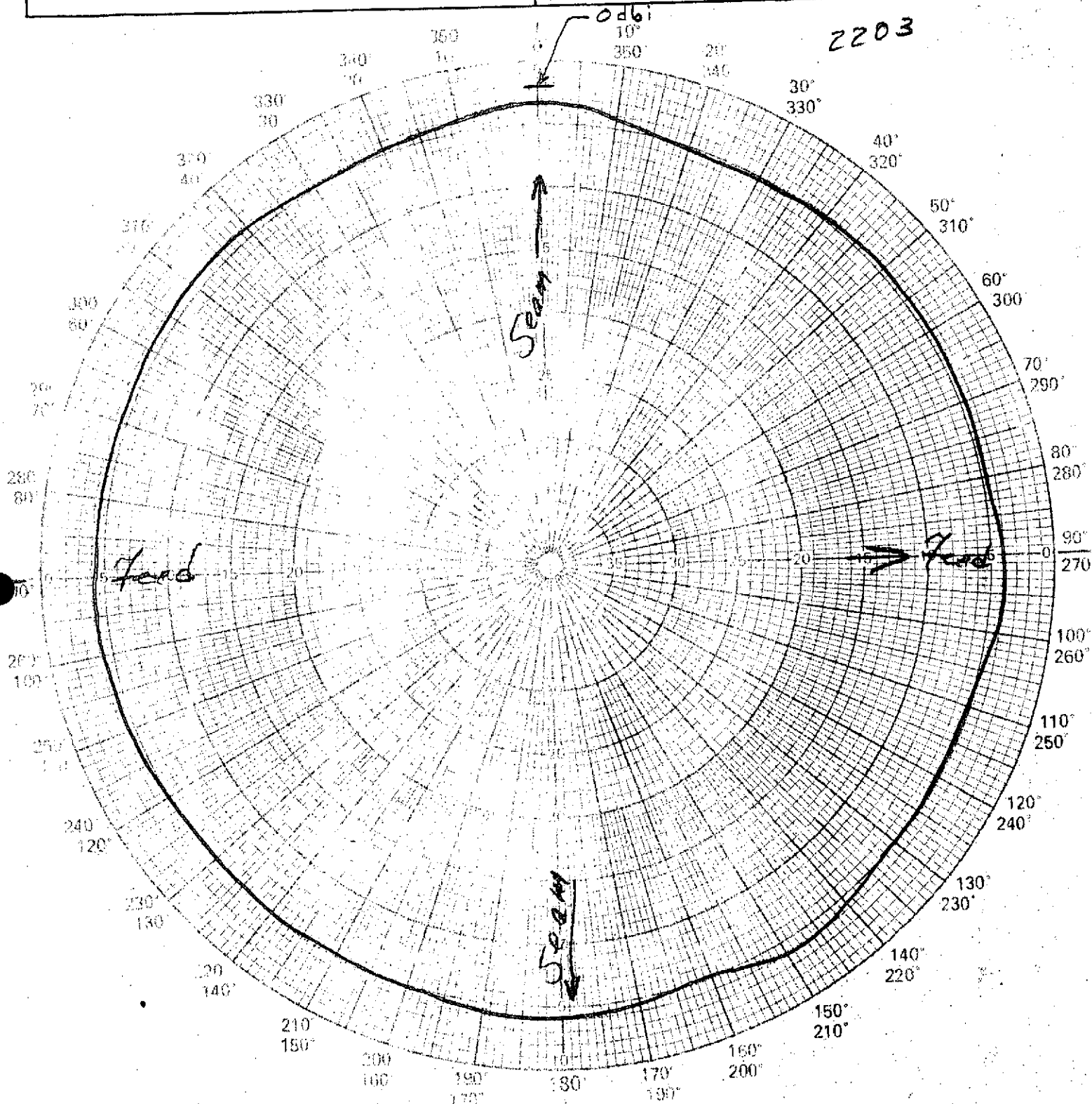
$Point = 6.6 @ 4.1 = 1.65$



WMSA  
5

REPORT NO. \_\_\_\_\_  
 MODEL SCALE Full  
 MODEL FREQUENCY \_\_\_\_\_  
 FULL SCALE FREQUENCY 2203  
 RANGE LOCATION \_\_\_\_\_

VEHICLE TYPE Proposal Mock up  
 ANTENNA Boards 3-26-1 and 3-26-2  
 SHEET \_\_\_\_\_ OF \_\_\_\_\_



PATTERN IN DB

**BALL BROTHERS RESEARCH CORPORATION**

REMARKS \_\_\_\_\_  
 \_\_\_\_\_  
 \_\_\_\_\_

POLARIZATION  $E\theta$    $E\phi$   RC  LC   
 $\phi = \text{Var}$   $\theta = 90^\circ$

OPER. \_\_\_\_\_ WITNESSED \_\_\_\_\_ DATE 3-29-4

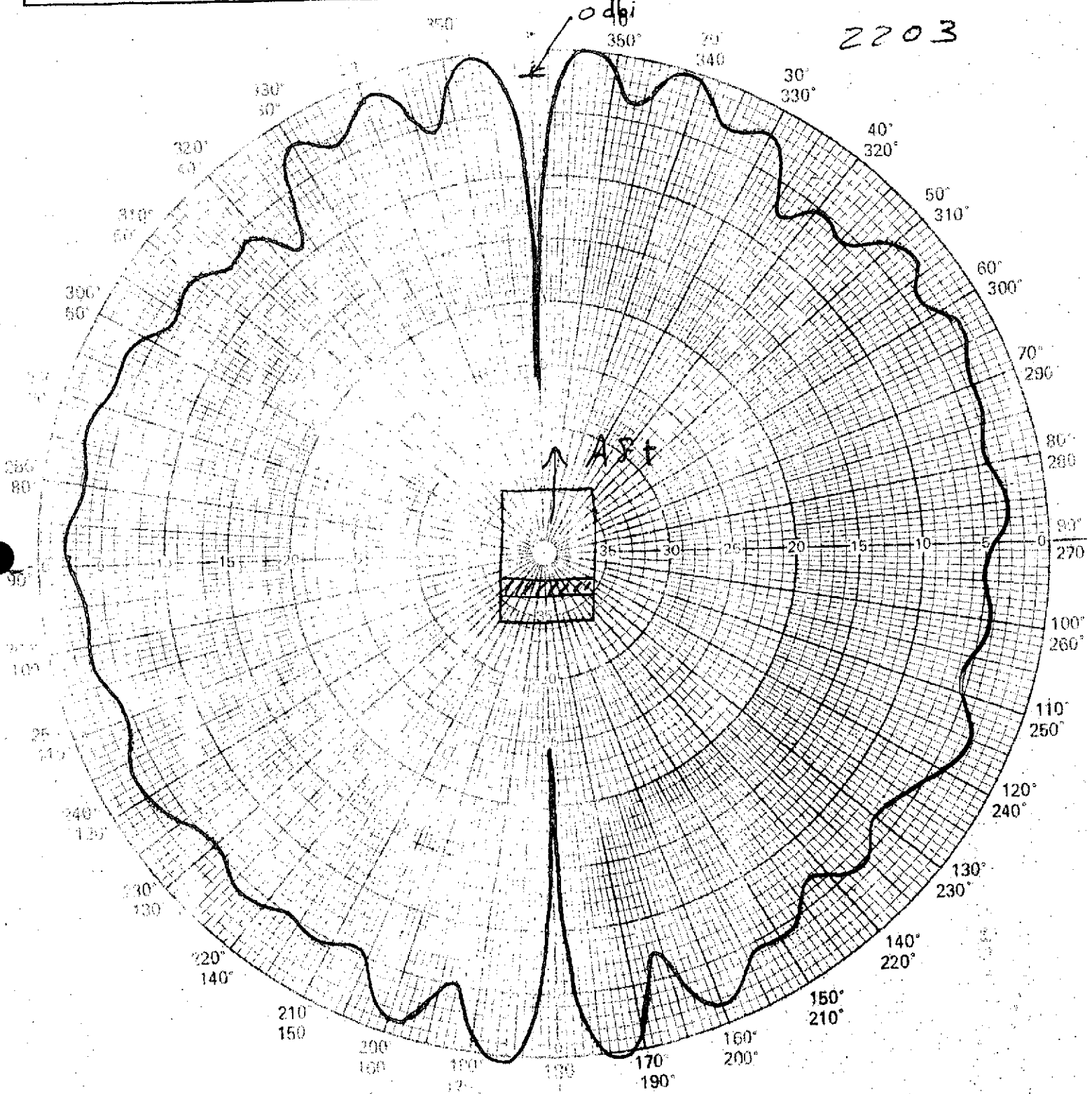
DB53-6  
3-70

Fig. 4 Roll Variation of Initial 2203.1 Antenna



REPORT NO. \_\_\_\_\_  
 MODEL SCALE Full  
 MODEL FREQUENCY \_\_\_\_\_  
 FULL SCALE FREQUENCY 2203  
 RANGE LOCATION \_\_\_\_\_

PROGRAM 360  
 VEHICLE TYPE Proposal Mockup  
 ANTENNA Bds 3-26-1 and 3-26-2  
 SHEET \_\_\_\_\_ OF \_\_\_\_\_



**PATTERN IN DB**

**BALL BROTHERS RESEARCH CORPORATION**

REMARKS _____ _____ _____	POLARIZATION $E\theta$ <input checked="" type="checkbox"/> $E\phi$ <input type="checkbox"/> RC <input type="checkbox"/> LC <input type="checkbox"/>
	$\phi = 0^\circ$ $\theta = \text{Var}$
	OPER. _____ WITNESSED _____ DATE <u>3-29-74</u>

Fig. 5 Aspect Radiation Pattern of Initial 2203.1 Antenna DB53-6  
5-70

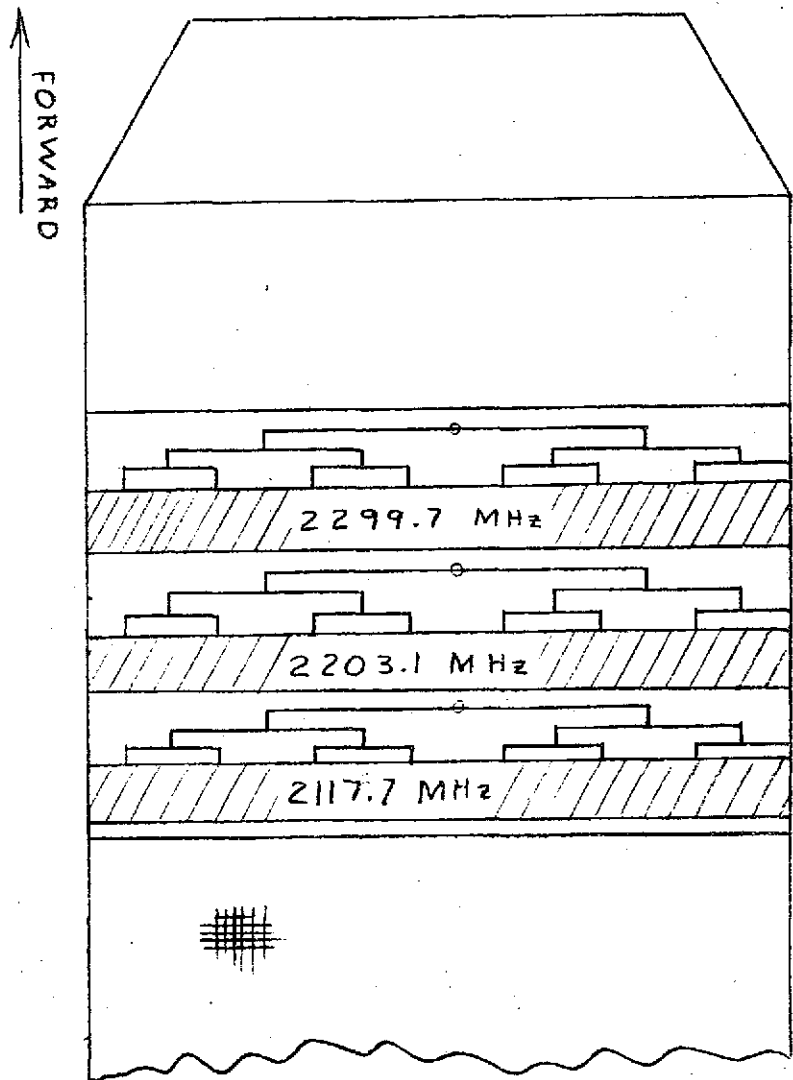


Fig. 6 Redshift Antenna Configuration



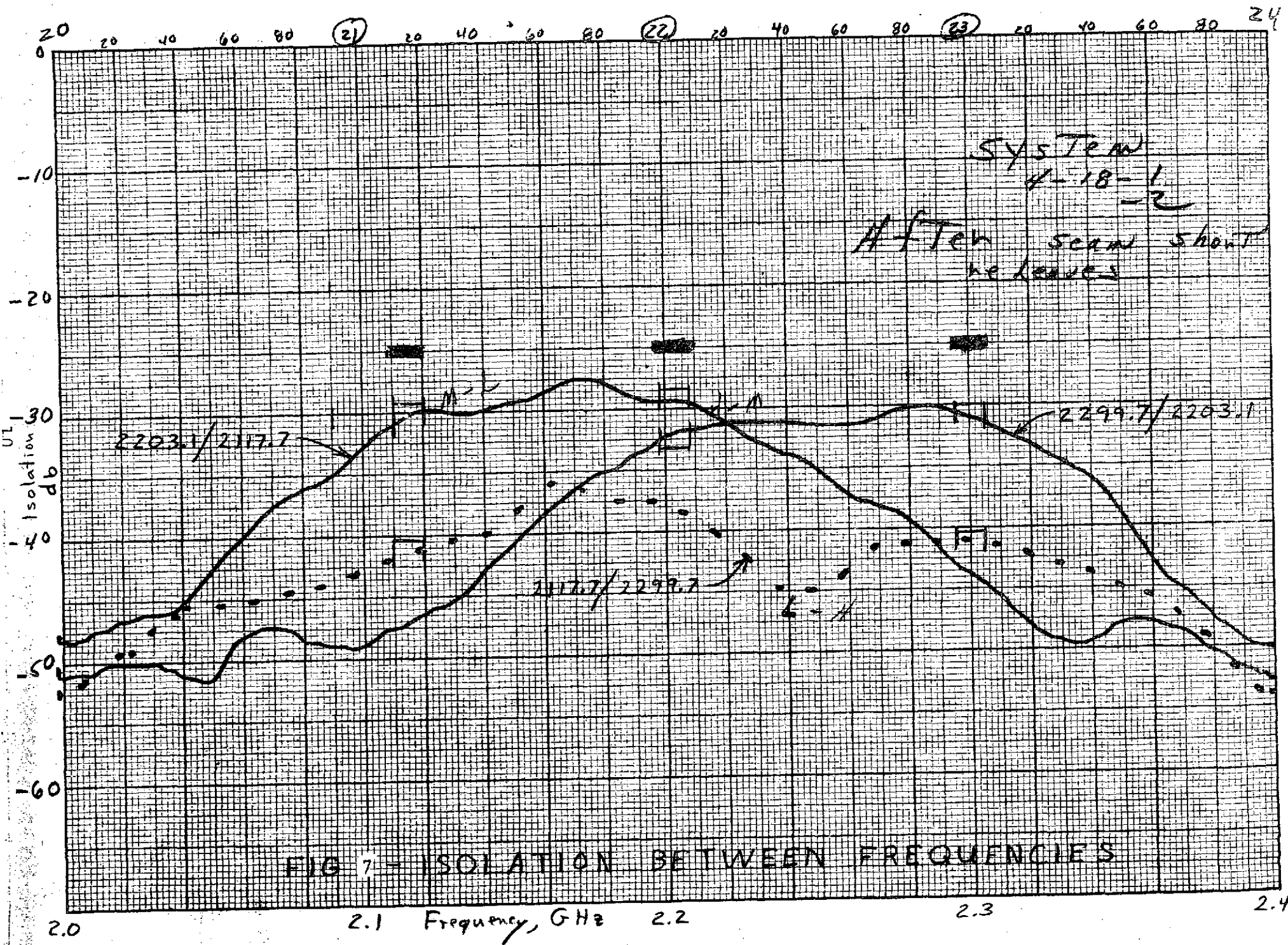


In this configuration the worst isolation is approximately 29 dB between the 2203.1 and 2117.7 MHz terminals. The isolation test results are shown in Fig. 7. It should be noted that the tested configurations where the antenna/feedline positions of one of the antennas was reversed the isolation between the antenna was at some points as low as -20 dB.

The configuration of Fig. 6 met the gain and phase specification for all frequencies, but the roll amplitude variation failed to meet specifications at certain angles. Tests were conducted to determine the sensitivity of the roll variation to the total test configuration. Figure 8 shows the roll amplitude variation measured as a result of the following modifications:

Effect of --	No.	Configuration Description
1. Adjacent Antennas	1a	3 antennas on standard ground plane. Model 4-8
	1b	Tested 2203 MHz. Other 2 antennas taped over.
2. Bumper slots in G.P.	2a	Same as (1b)
	2b	Taped over slots with aluminum tape
3. Open aft end of G.P.	3a	Same as (2b)
	3b	Ground plane filled with absorber material
4. Wire mesh relative to solid ground plane	4a	Same as (3b)
	4b	Wire mesh covered with aluminum foil

The only significant variation occurred between 1a and 1b when the antennas adjacent to the center 2203.1 MHz antenna were covered with aluminum tape.





The measurements of Fig. 8 were made because the roll amplitude patterns seemed to be punctuated at the feed point location and at the seams between the two antenna sections. After various possible causes such as antenna soundness and seam dimensions were investigated, transformer lines were placed on the feed lines which fed the area between the feed point location and the seam (Fig. 9). It was thought that the proximity of the feed lines had caused a slight unbalance of the power to this area of the antenna. The transformers would increase the power and balance the roll amplitude. The assumption proved to be correct and was incorporated into the final network.

Figures 10 and 11 show the fabrication of the deliverable antenna S/N 001 antenna. S/N 002 was fabricated in a like manner. The final measurement data on these antennas was sent with the delivered units. The performance of the delivered antennas was quite satisfactory and well within specifications.

#### B. Phase/Temperature Measurements and Analysis

During the development phase and amplitude measurements were taken over the temperature range from 20°C to -10°C. Results showed that the relative phase variation in each conical cut were within the specified 45° limitation, and that the relative phase variation changes very little with temperature. However, the absolute phase changed significantly over the 30° temperature range. As expected, the magnitude of the phase variation is directly proportional to the amplitude variation. The absolute phase variation was magnified somewhat by the fact that the test chamber rotary joint and test cable also experienced some cooling. In addition, the antenna surface probably had some condensation build-up during the test. The condensation would affect the radiated phase. Figure 12 illustrates the temperature test chamber. Since the thermal enclosure had no window, we could not observe how much

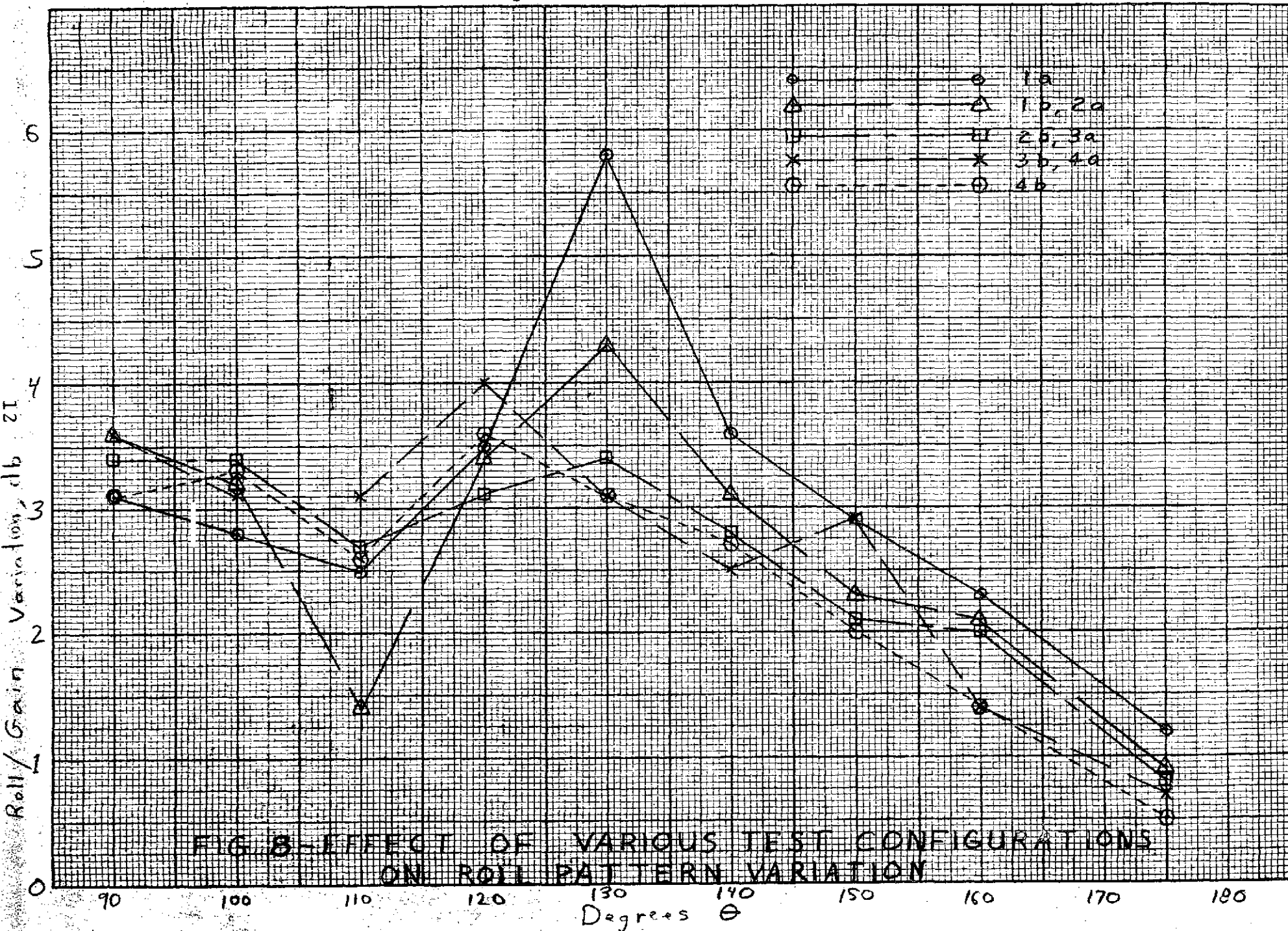


FIG. 8 - EFFECT OF VARIOUS TEST CONFIGURATIONS ON ROLL PATTERN VARIATION

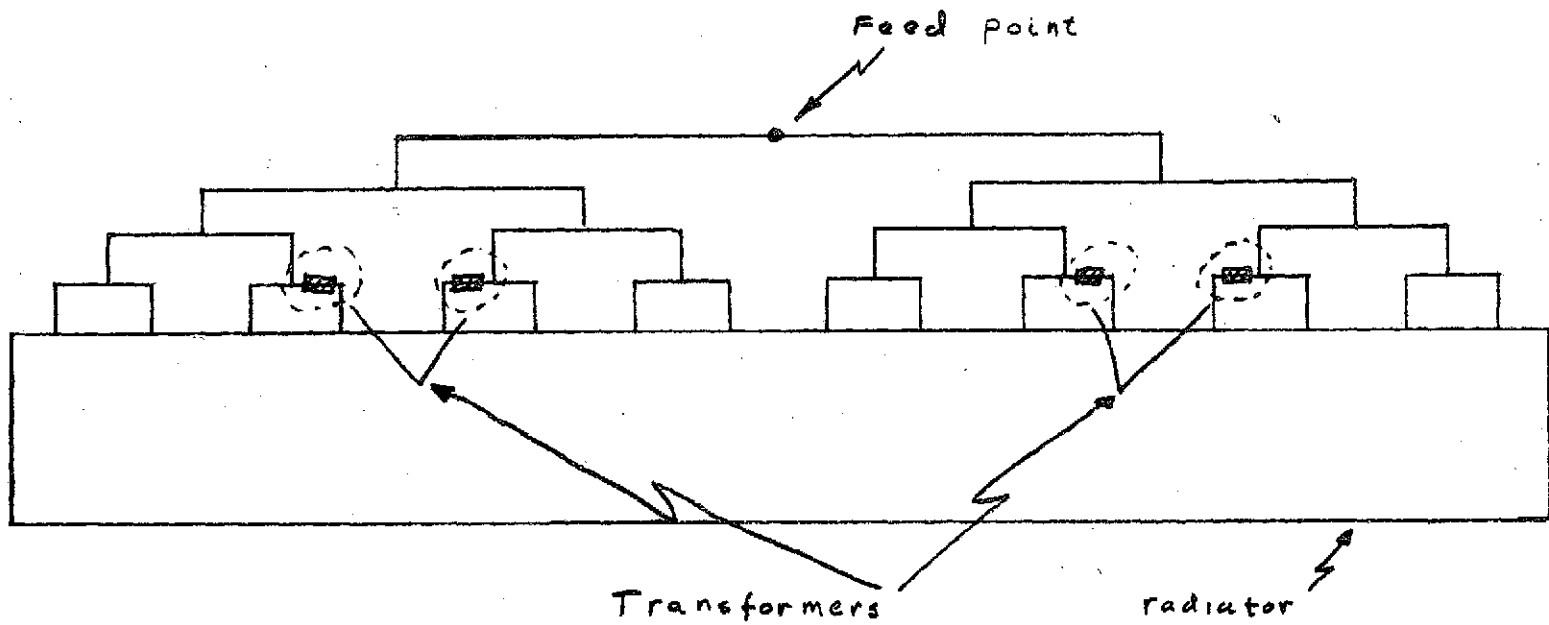


Fig. 9 Positioning of Feed Line Transforme for Power Equalization

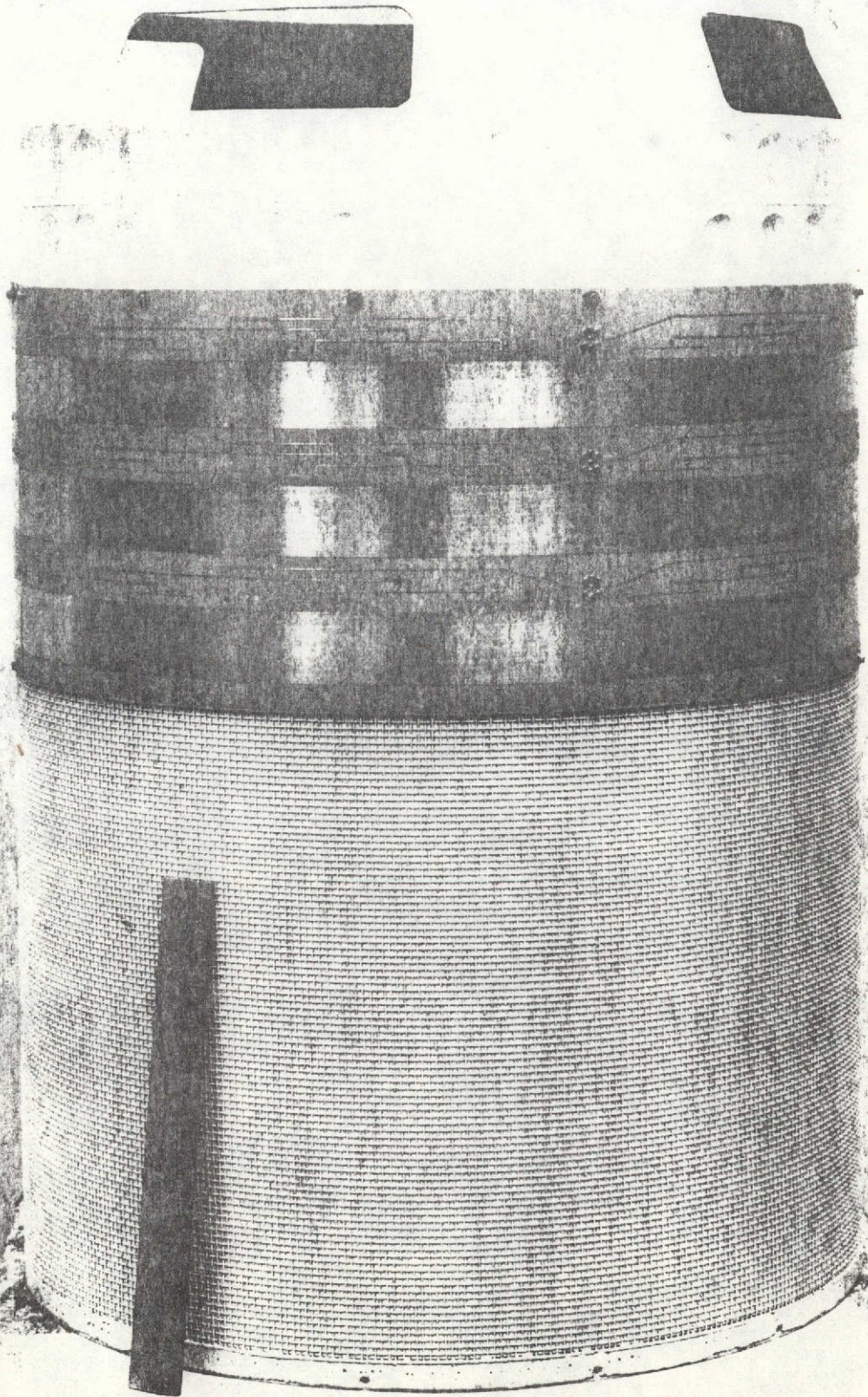


Fig. 10 Antenna Model SN/001



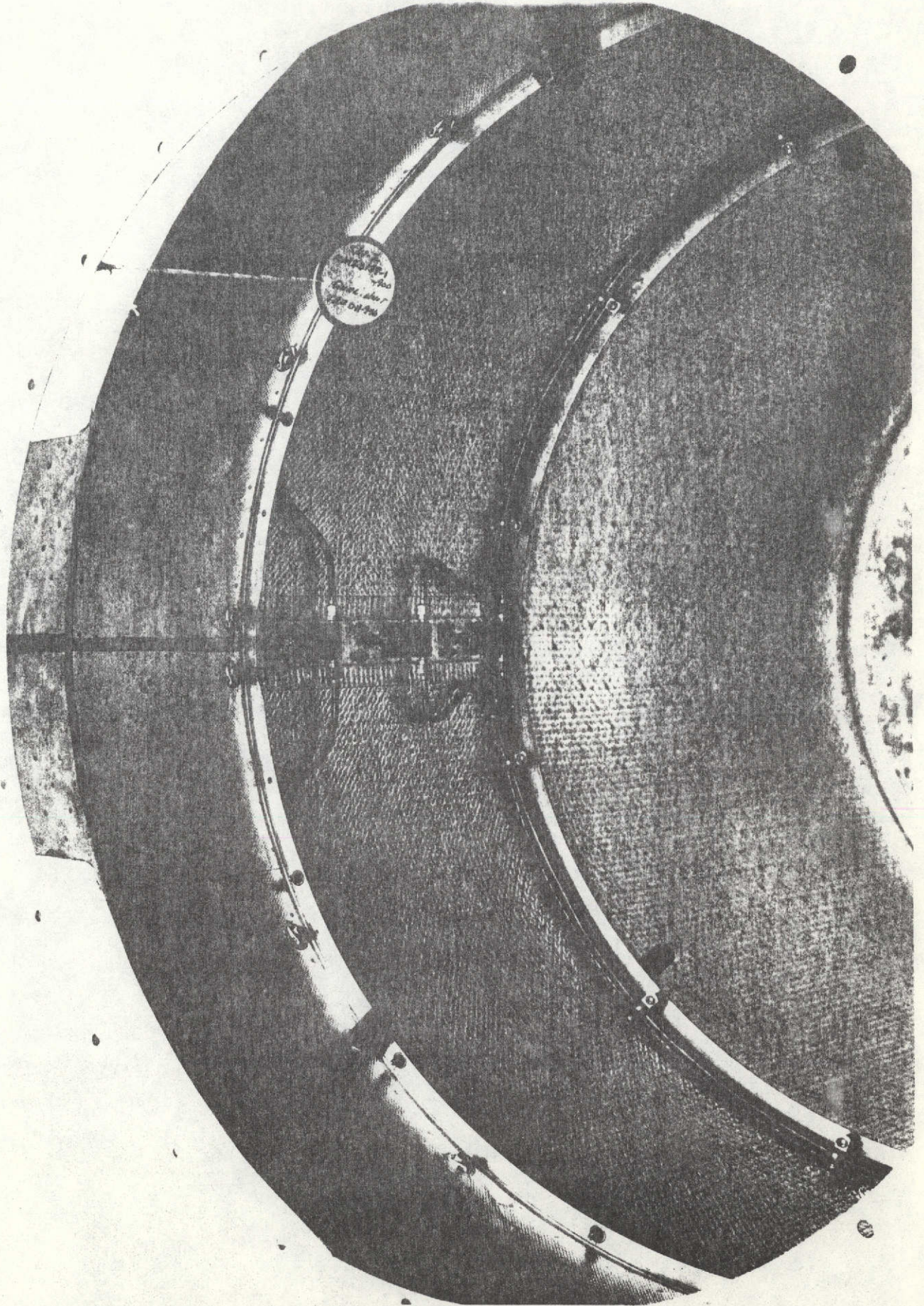


Fig. 11 Feed Cables and Power Dividers Antenna SN/001

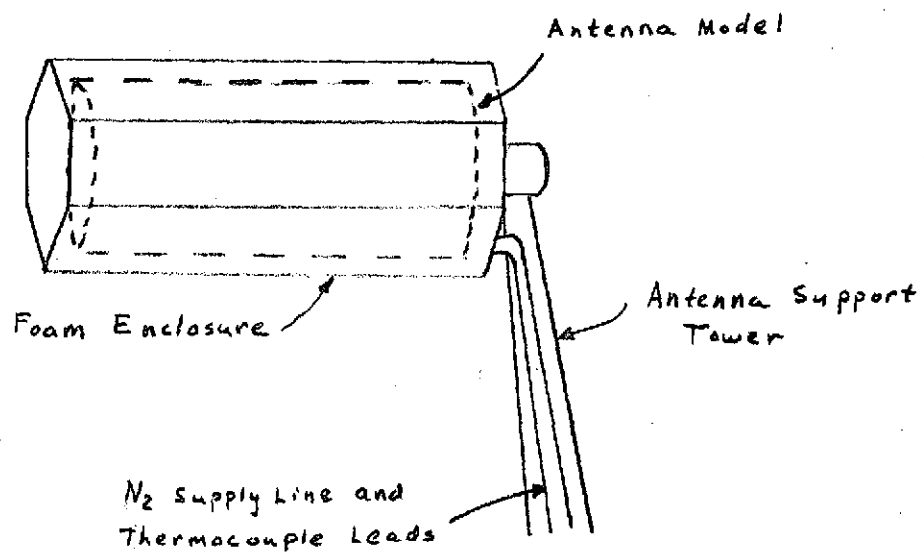


Fig. 12 Phase/Amplitude 30° Temperature Test Chamber



condensation was present during the test.

In a related effort, tests were made for the analysis effort to predict the total system phase change from  $-100^{\circ}\text{C}$  to  $125^{\circ}\text{C}$ . Separate tests were performed to measure the phase change in the power dividers, cables and connectors, feed networks on the PC board and a radiating patch by itself. During the testing of the section of the radiating antenna, as in the full antenna tests, some condensation formed on the antenna surface at temperatures close to  $0^{\circ}\text{C}$ . Coincidentally, the rate of phase change increased significantly around the  $0^{\circ}\text{C}$  range. The rate of change of phase remained quite linear over the rest of the temperature range. The system phase analysis report titled "Analysis of the Phase Variation Resulting from Temperature Variation of the Redshift Antenna", is attached as an addendum to this report.

### C. Temperature Survivability Test

Temperature survivability test were performed on a development antenna and the results were presented at the CDR. There was essentially no change in VSWR between the pre and post temperature tests. However, the roll pattern amplitude variation at one conical cut ( $\theta=135^{\circ}$ ) at 2117 MHz increased from a 3.25 dB variation to 4.5 dB from the pre to post temperature tests. This antenna was not mounted in the flight configuration. This situation was discussed at the CDR and it was decided to rerun the test.

Figures 13 and 14 illustrate the variation of the roll patterns and VSWR of the antenna SN 001 before and after the repeat of the temperature survival test ( $-80^{\circ}\text{C}$  to  $+50^{\circ}\text{C}$ ). The VSWR showed a minor shifting of the impedance curve. The roll pattern variation versus aspect angle seemed to become smoother. The temperature cycling seemed to set the antenna to the curvature of the model and reduce the peak variation of the roll pattern variation.

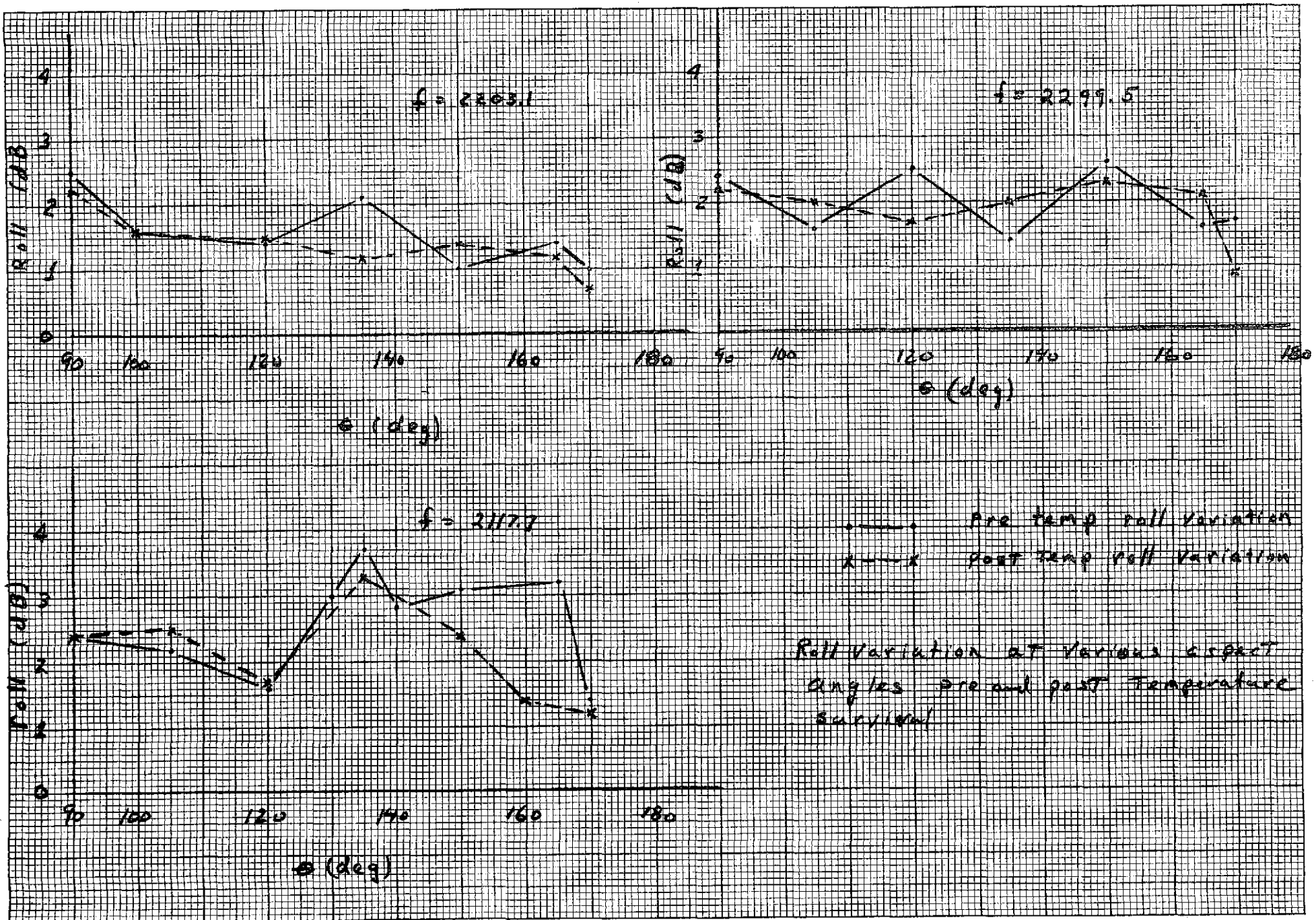


Fig. 13 Pre and Post Temperature Survivability Test - Roll Variation

19

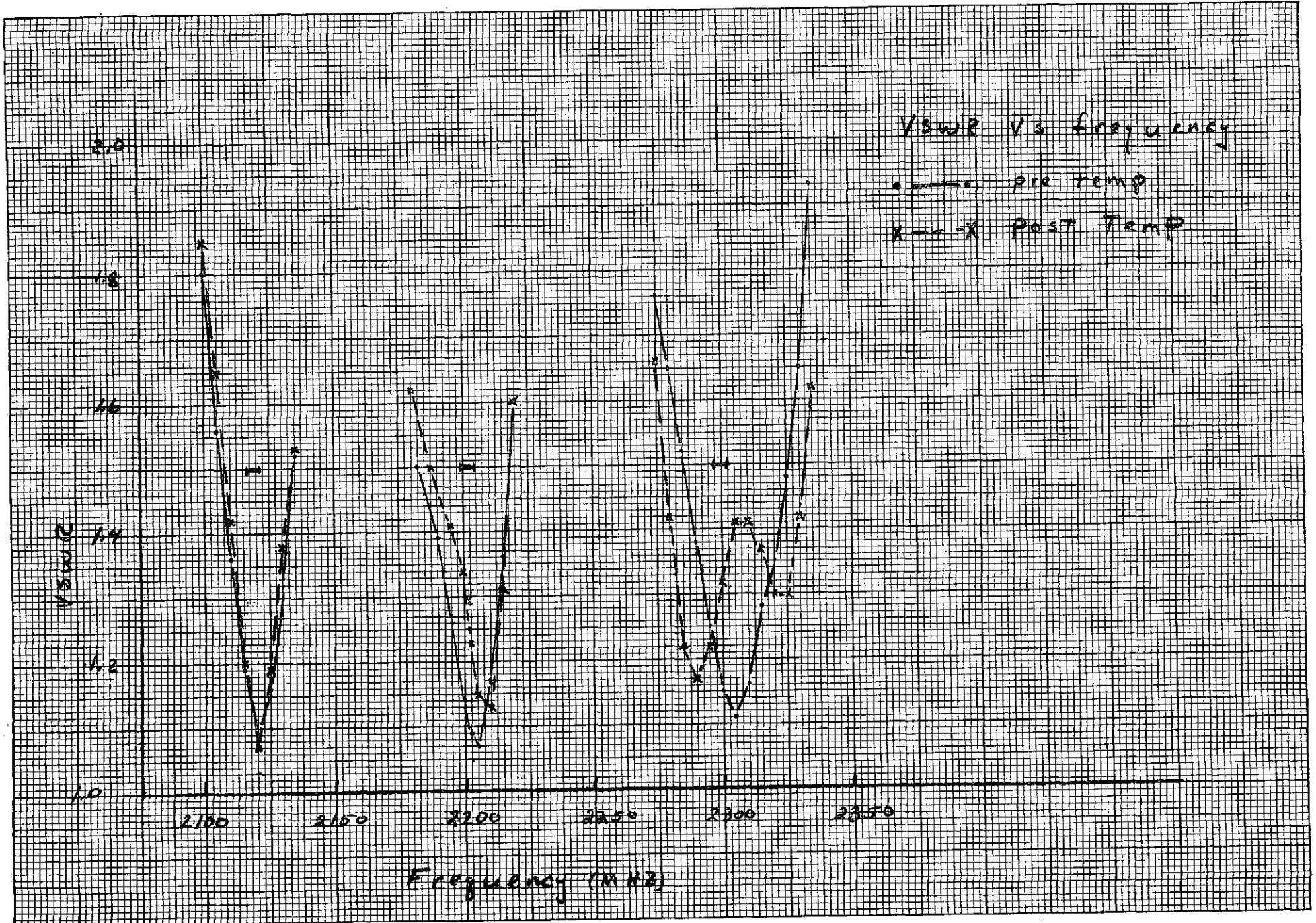


Fig. 14 Pre and Post Temperature Survivability Test - VSWR



#### D. Conclusions

The major items which affected the successful completion of this antenna within specification can be listed as follows:

- Accurate and symmetrical feedline lengths such that the antenna is fed with very uniform and equal phase.
- Roundness. The roll amplitude variation patterns are affected by the roundness of the ground plane and the conforming of the antenna to the ground plane.
- Isolation. Best isolation is dependent upon the radiating elements and separation. Therefore, the feedline - radiator, feedline - radiation etc., arrangement maximizes the isolation.
- The proximity of feedlines and weak coupling between feedlines may cause an unbalancing of the amplitude around the antenna. This unbalancing may be compensated for by transforming sections which increase the power to areas of the roll pattern which show reduced power.

Additionally, the phase variation of the antenna system with temperature is quite linear. The phase variation of the microstrip feedlines tended to decrease in slope at temperatures above 50°C. Since the microstrip lines are a primary phase determining factor in the antenna system, the slope of the phase variation of the antenna system also tends to decrease at the temperatures above 50°C. A phase step occurred in the phase analysis measurements for the radiating antenna between the temperatures of +10°C and -10°C. This step was caused by the condensation of water on the antenna surface. This condition should not occur in a flight environment.



ADDENDUM 1

ANALYSIS OF THE PHASE VARIATION RESULTING FROM  
TEMPERATURE VARIATION OF THE REDSHIFT ANTENNA



ANALYSIS OF THE  
PHASE VARIATION RESULTING FROM  
TEMPERATURE VARIATION  
OF THE REDSHIFT ANTENNA

Project 3260

18 June 1974

Contract NAS8-29504

Submitted to

NASA/MSFC

By

BALL BROTHERS RESEARCH CORPORATION  
BOULDER, COLORADO





## PHASE/TEMPERATURE ANALYSIS OF THE REDSHIFT ANTENNA

### 1.0 INTRODUCTION

The phase/temperature analysis of the Redshift Antenna consists of actual measurements of individual components of the antenna. The phase/temperature measurements were separated into four (4) separate tests:

- $\Delta\phi/\Delta T$  of coaxial cables
- $\Delta\phi/\Delta T$  of coaxial cables and power divider
- $\Delta\phi/\Delta T$  of microstrip transmission line
- $\Delta\phi/\Delta T$  of microstrip antenna segment

These measurements are backed by computation where the pertinent information is available. The total value of phase change versus temperature is calculated by summation of the separate values. The effects of the temperature on the radiating cavity were measured by varying the temperature of an antenna segment and recording the transmitted phase. The major problem in the measurement of the radiating cavity is the phase change caused by condensation on the face of the antenna.

### 2.0 TEST RESULTS

#### 2.1 $\Delta\phi/\Delta T$ OF COAXIAL CABLES

The test setup for coax cables for both the high and low temperature ranges is shown in Fig. 1. During the high temperature test the coaxial cables were placed in an enclosed oven and the cable temperature monitored by a thermocouple. The low temperature range phase variation was measured by placing the coaxial cable

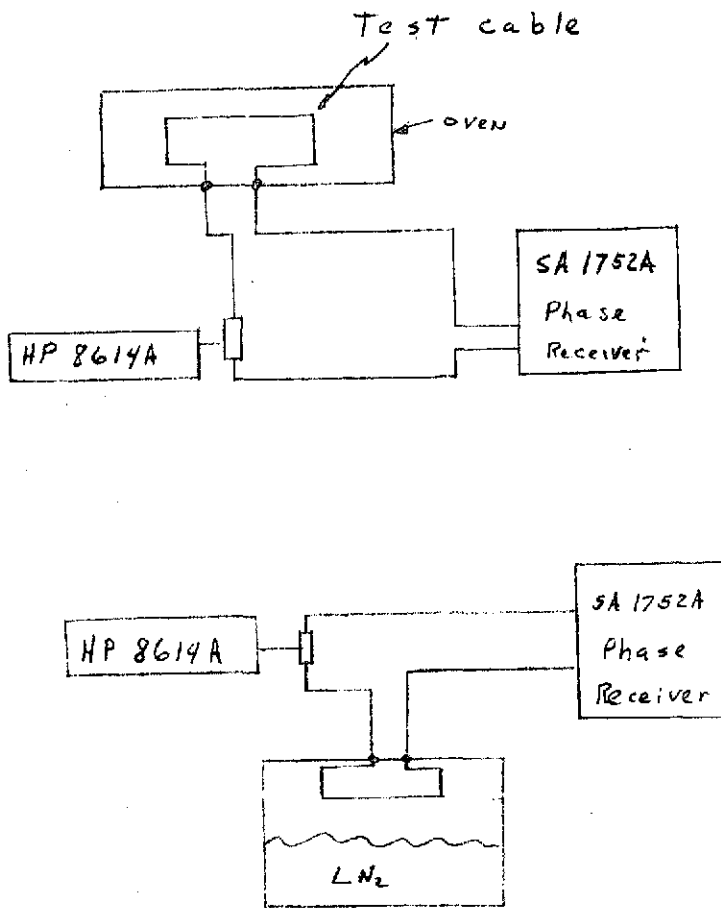


Fig. 1 Coaxial Cable  $\Delta\phi/\Delta T$  Test Setup for High and Low Temperature Ranges



length above an insulated receptacle of liquid nitrogen. The phase variation was monitored as the temperature decreased. However, since the downward temperature change was quite rapid, the cables were placed in an insulated box and the phase/temperature monitored as the temperature rose. This procedure allowed more data points to be obtained.

Figure 2 shows the recorded phase variation of the 34-inch length of coaxial cable. Between plus and minus 40°C the slope of the phase change with temperature was the most rapid—approximately 10 degrees phase per 80 degrees centigrade for 34-inches of coax ( $.0037^\circ\phi/^\circ\text{C}/\text{inch}$ ). The slope of the phase change was much less for temperature extremes beyond these temperatures. Figure 2 also relates the calculated cable phase change using the manufacturer's representative numbers of -15 ppm/°C for the high temperature range and -55 ppm/°C in the low temperature range to -40°C. It is important to note that both curves demonstrate a similar change in slope.

## 2.2 $\Delta\phi/\Delta T$ OF COAXIAL CABLES AND POWER DIVIDERS

Figure 3 illustrates the test setup for the measurement of the phase/temperature variation of the coaxial cables and power divider. The test procedure was similar to that of the coaxial cable except for the addition of the power divider and a length of cable with a matched load. Energy was fed into the power divider in a fashion similar to the flight operation. The additional coaxial cable and matched load provided a matched load to the unused power divider port. During the temperature test the coaxial cable allowed the matched load to be placed outside of the temperature variation.

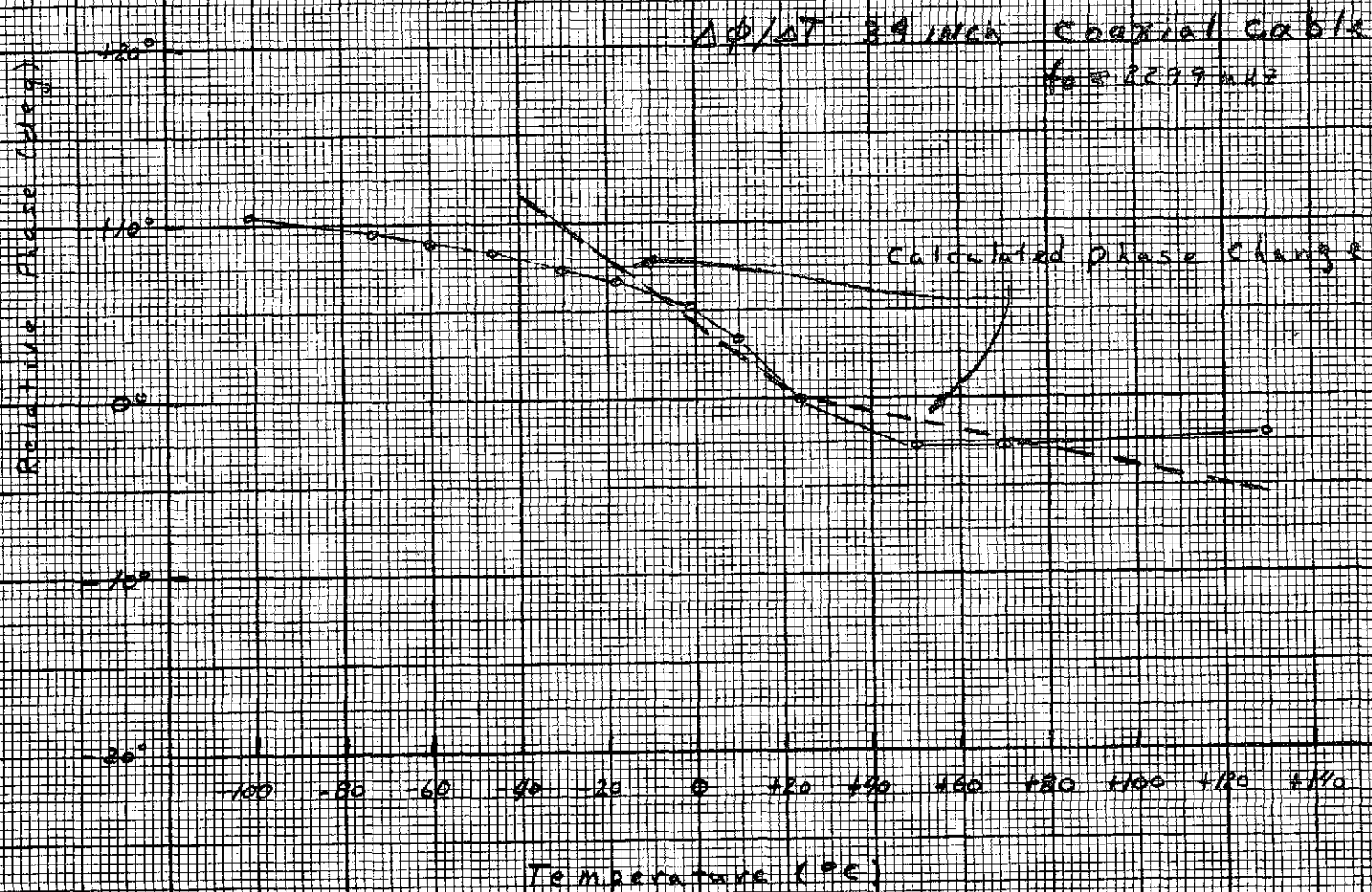


Fig. 2 Measured  $\Delta\phi/\Delta T$  for 34-inch Length of Coaxial Cable

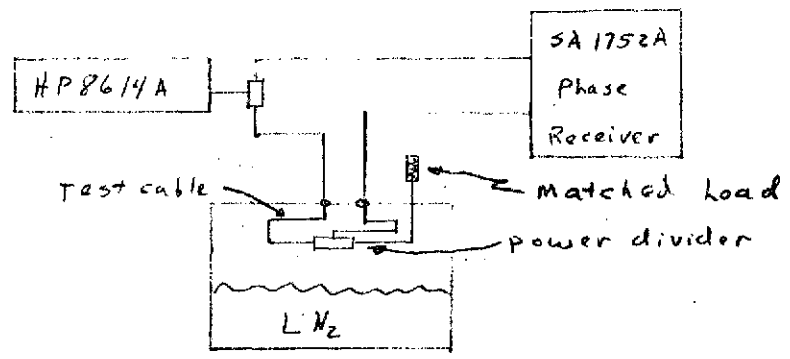
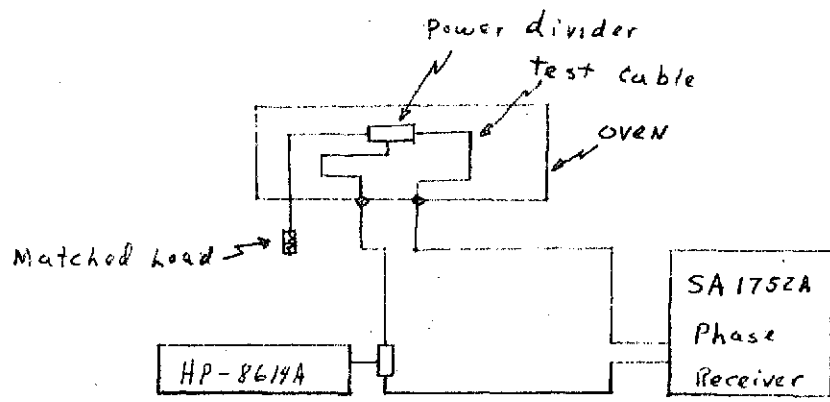


Fig. 3 Power Divider  $\Delta\phi/\Delta T$  Test Setup for High and Low



Figure 4 shows the results of the phase/temperature measurements. The results are quite similar to those obtained in Section 2.1 for the coaxial cables alone. This result is quite logical since the same coax cable was used and the only difference is the additional small length of the power divider. Figure 5, the difference between the results in Figs. 4 and 2 is the change due to the power divider alone.

### 2.3 $\Delta\phi/\Delta R$ OF MICROSTRIP TRANSMISSION LINE

The test setup for the phase/temperature testing of the microstrip transmission line is the same as the coaxial cable in Fig. 1. The physical length of the microstrip transmission line was nine inches. This line was an actual Redshift transmission line printed on the pcb with a connector attached at each end.

Figure 6 shows the phase variation with temperature. The phase/temperature variation is somewhat larger than the coax cable .0098/°C/inch versus .0037/°C/inch for the plus 40°C to minus 40°C range. However, similar to the coaxial cable, the slope of the phase/temperature decreases at the temperature extremes. At the high temperature extreme (+80 - +125°C) the phase change reversed direction.

### 2.4 $\Delta\phi/\Delta T$ OF MICROSTRIP ANTENNA SEGMENT

Figure 7 illustrates the test setup for the phase/temperature testing of a section of the antenna. The antenna and receiving horn were surrounded with absorber to assure that the phase was not affected by exterior reflections. The antenna was mounted on an aluminum plate which acted as a heat sink to provide a slow transition of temperature of the antenna. The temperature

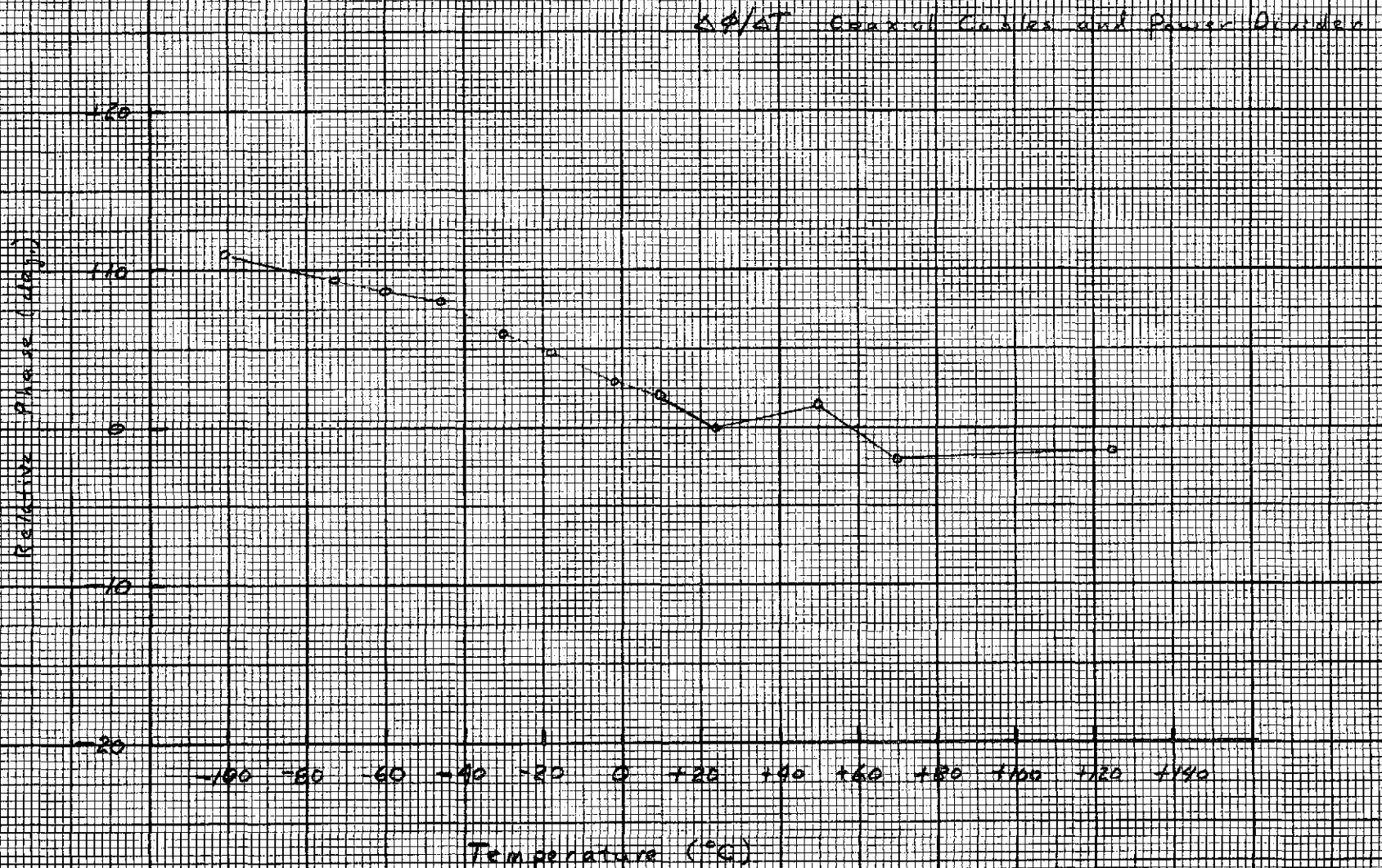


Fig. 4 Measured  $\Delta\phi/\Delta T$  of Power Divider and 34-inch Coaxial Cable

6

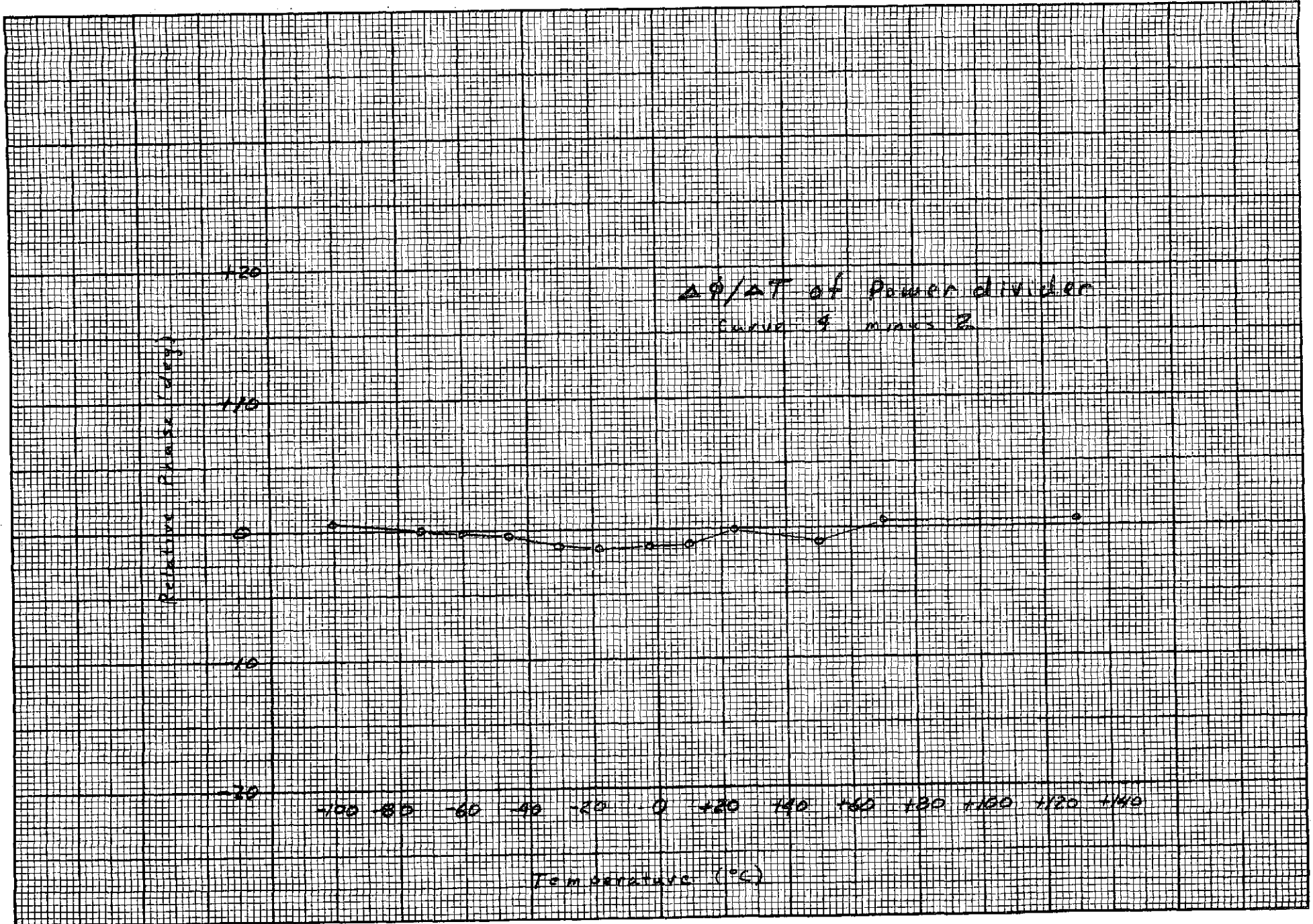


Fig. 5  $\Delta\phi/\Delta T$  of Power Divider (Fig. 4 minus Fig. 2)



10

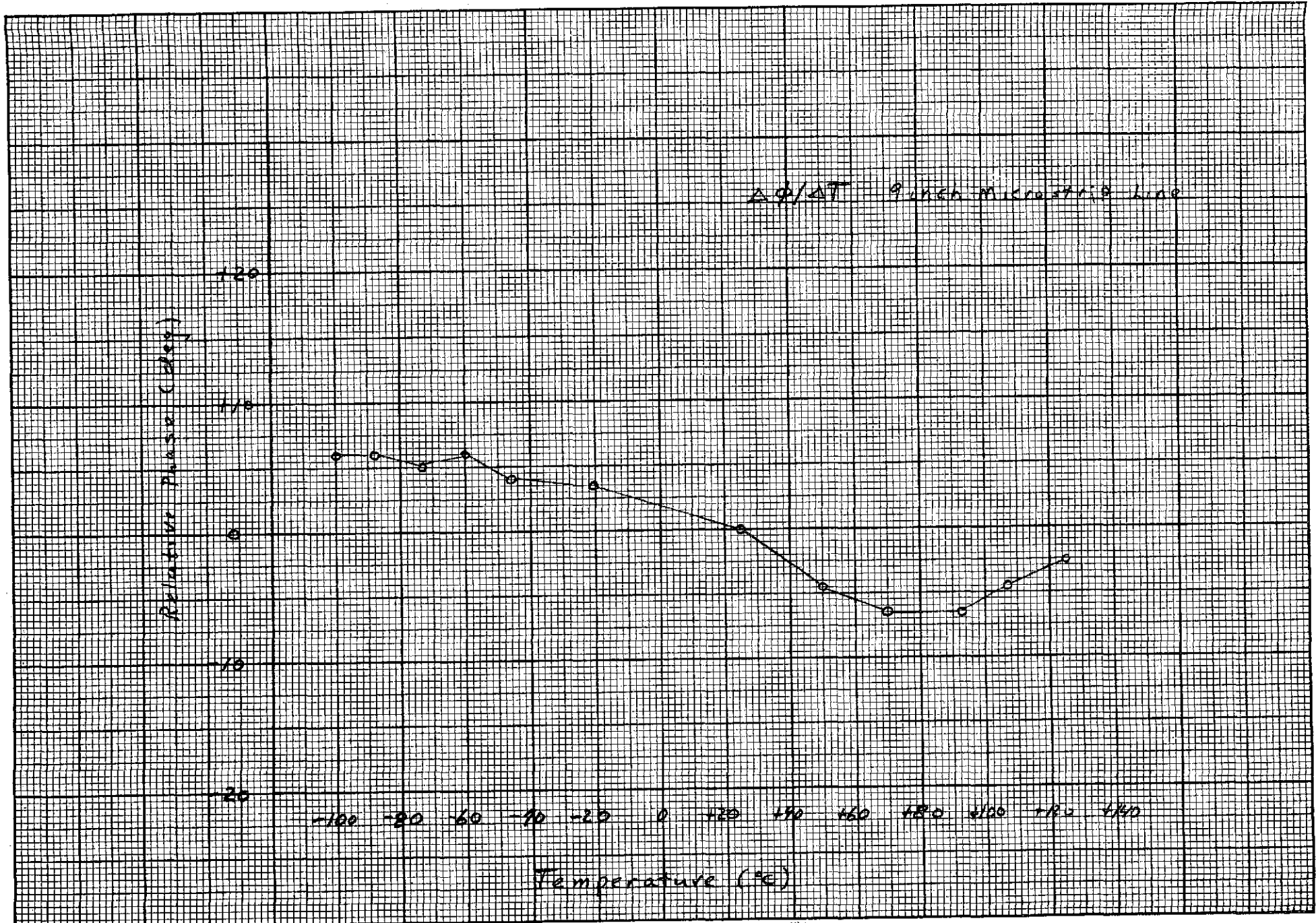


Fig. 6 Measured  $\Delta\phi/\Delta T$  of 9-inch Microstrip Line

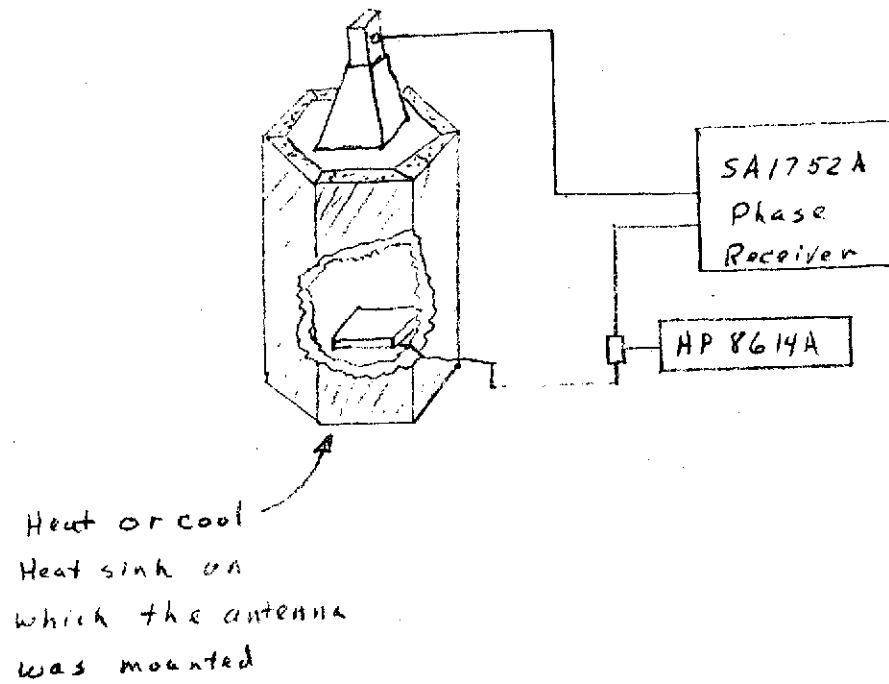


Fig. 7 Test Setup for Measurement of  $\Delta\phi/\Delta T$  of Antenna Segment



thermocouple was placed on the antenna front surface. The high temperature range was measured by applying a heat gun to the surface of the aluminum plate. The antenna was cooled by placing the antenna over the surface of a receptacle of liquid nitrogen.

A prime difficulty in the measurement of the phase/temperature variation of the antenna was a step variation of phase which occurred as the antenna was cooled. As the temperature was lowered from 24 to 10°C, a dew formed on the surface of the antenna and a rapid change in phase occurred. The test continued down to -100°C, and the phase/temperature measurements were repeated as the antenna was allowed to return to ambient room temperature. The final phase at 24°C did not agree with the initial phase measurements. The dew was removed from the surface of the antenna with a soft paper towel and the phase changed by 19° returning to the initial phase measurement. Attempts to set the antenna in the fumes of the liquid nitrogen to prevent condensation were not successful. Figure 8 shows the phase versus temperature variation with the condensation. The slope of the phase/temperature curves are basically the same for the high and low temperature ranges outside of the region where the frost or dew occurred on the antenna. Figure 9 is a phase/temperature curve of Fig. 8 with the 19° phase step removed. In the absence of an air/water atmosphere it would be correct to use the phase/temperature curve of Fig. 9 for the system phase calculations.

### 3.0 CALCULATED SYSTEM $\Delta\phi/\Delta T$

The calculated system  $\Delta\phi/\Delta T$  is a summation of the phase change with temperature of the individual components. The  $\Delta\phi/\Delta T$  of the antenna (Fig. 9) and the power divider (Fig. 5) are representative of the actual components. The  $\Delta\phi/\Delta T$  for the coaxial cable and the microstrip transmission line were calculated from the 34-inch and 9-inch length samples tested.

13

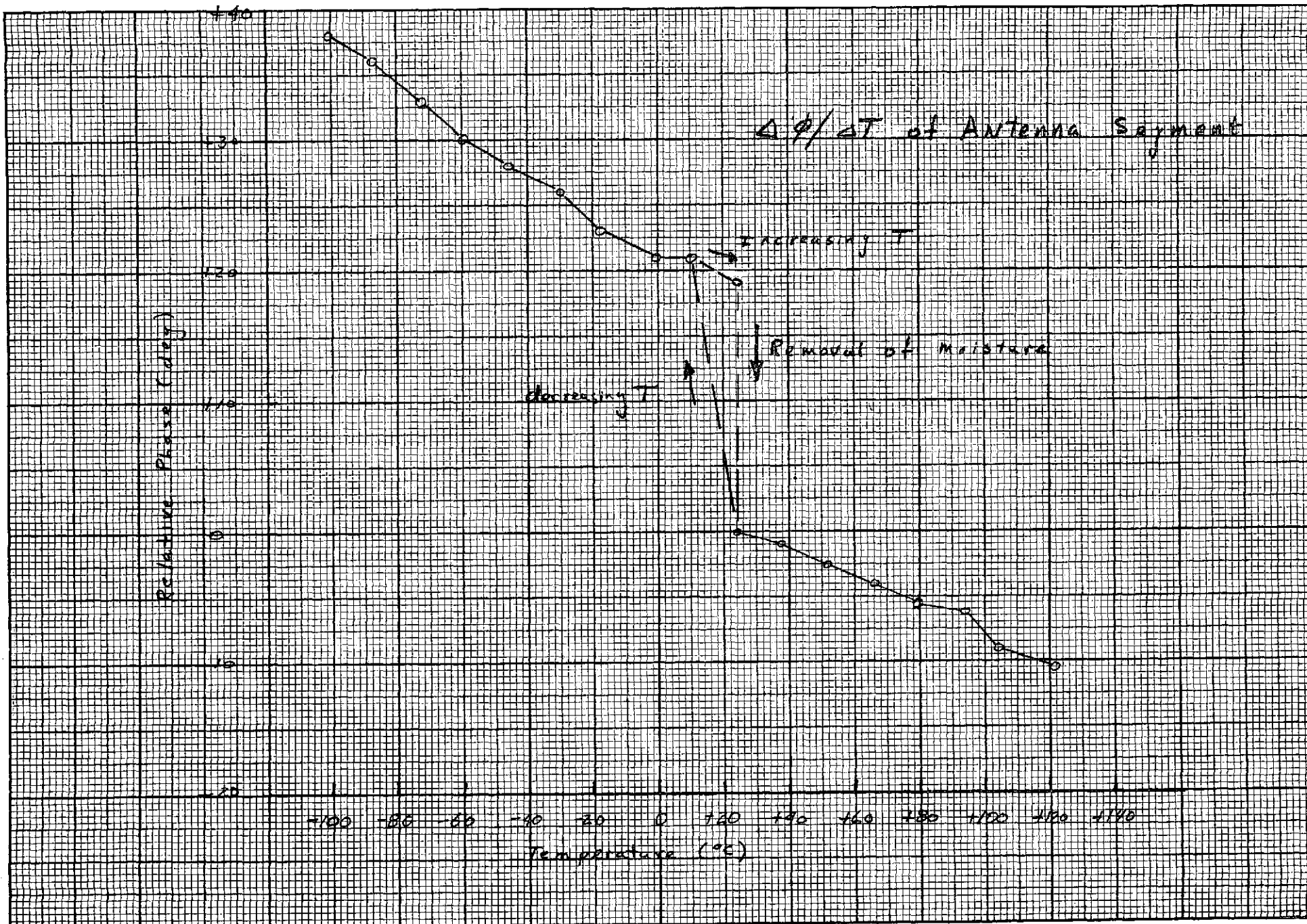


Fig. 8 Measured  $\Delta\phi/\Delta T$  of Antenna Segment

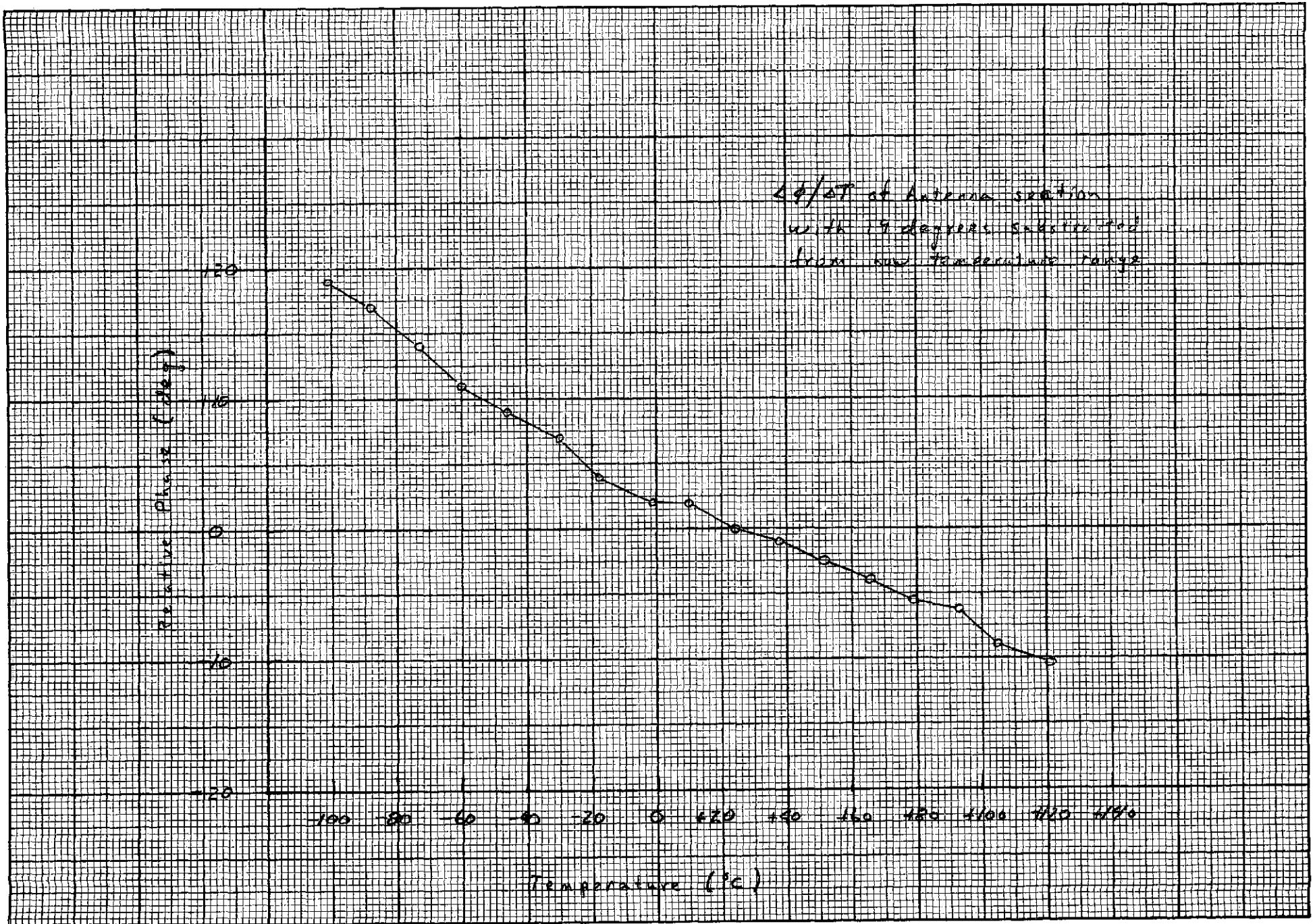


Fig. 9 Modified  $\Delta\phi/\Delta T$  of Antenna Segment



Figure 10 shows the  $\Delta\phi/\Delta T$  of the 20.5 inch (longest) length coaxial cable. The Redshift microstrip transmission line length from the coaxial terminal to the point where the antenna segment was tested is 17.95 inch and the extrapolated  $\Delta\phi/\Delta T$  is shown in Fig. 11. Figure 12 is the summation of Figs. 5, 9, 10 and 11 which is the calculated system  $\Delta\phi/\Delta T$  with the modified antenna segment  $\Delta\phi/\Delta T$ . The  $\Delta\phi/\Delta T$  slope is approximately  $0.286^\circ/^\circ\text{C}$  from  $-100^\circ\text{C}$  to  $+10^\circ\text{C}$  and approximately  $0.625^\circ/^\circ\text{C}$  from  $+10^\circ\text{C}$  to  $+50^\circ\text{C}$ . The phase tends to be almost constant for the temperature variation above  $+50^\circ\text{C}$ . Although Section 2.4 explained the reason for the modified antenna  $\Delta\phi/\Delta T$  curve, the system  $\Delta\phi/\Delta T$  with the unmodified curve is shown in Fig. 13. Figure 14 relates the modified  $\Delta\phi/\Delta T$  with 17-inch cables.

#### 4.0 COMPARISON WITH FULL-MODEL TESTS

The phase changes predicted above appear to correlate quite well with the test data obtained by testing the complete antenna over a  $30^\circ\text{C}$  range.

The enclosure used in the full-model phase tests was designed so that no moisture would condense on the enclosure. However, immediately following the temperature tests on the 2203 MHz frequency, it was noted that considerable condensation existed on the antenna itself. The actual amount of condensation on the antenna during test could not be observed because of the construction of the thermal enclosure. The phase meter was zeroed prior to taking each roll pattern, and the average phase difference between  $20^\circ\text{C}$  and  $-10^\circ\text{C}$  for each of the three pairs of roll patterns taken at 2203 MHz was  $36^\circ \phi$ .

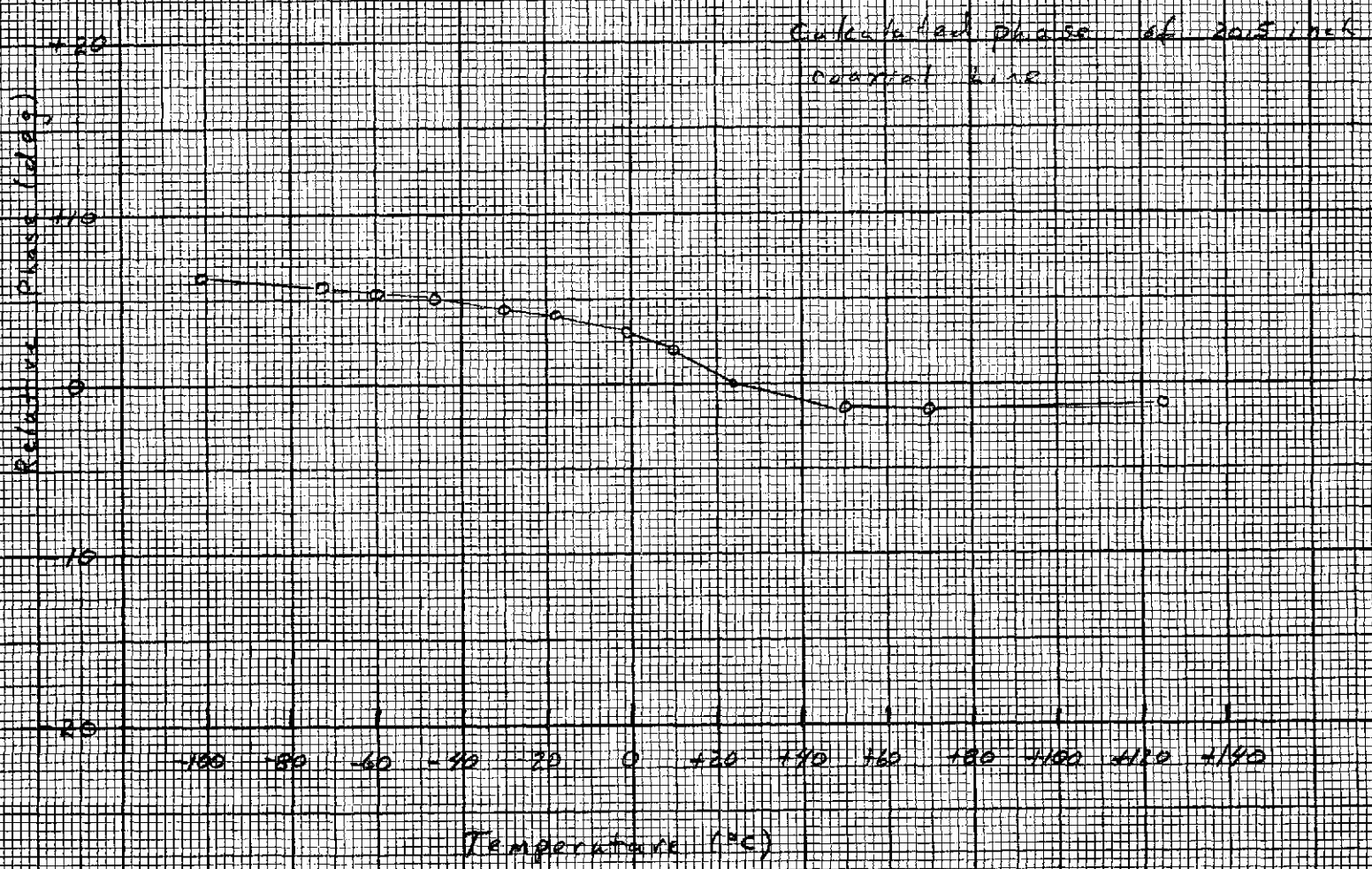


Fig. 10 Extrapolated  $\Delta\phi/\Delta T$  of 20.5-inch coaxial cable

17

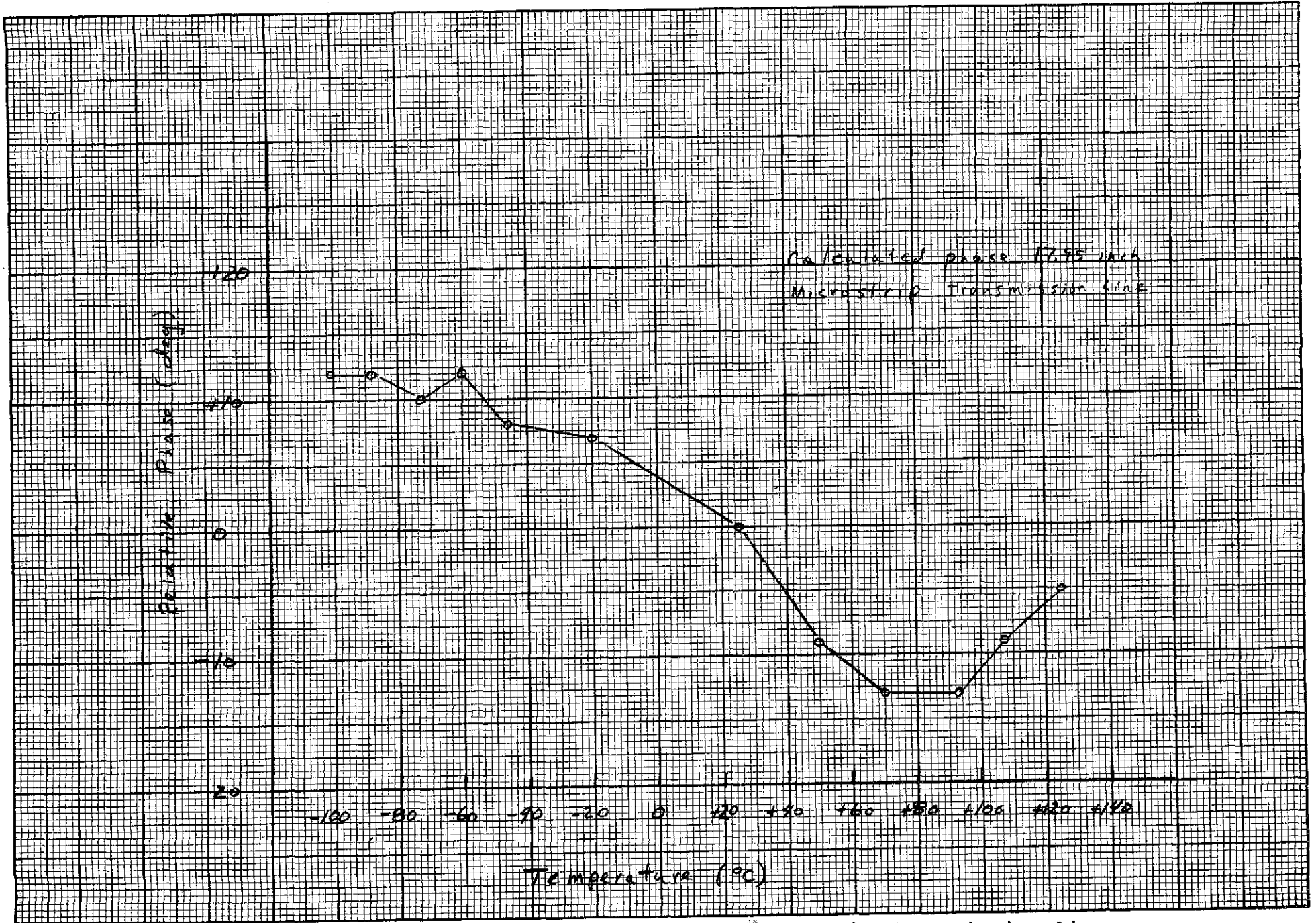
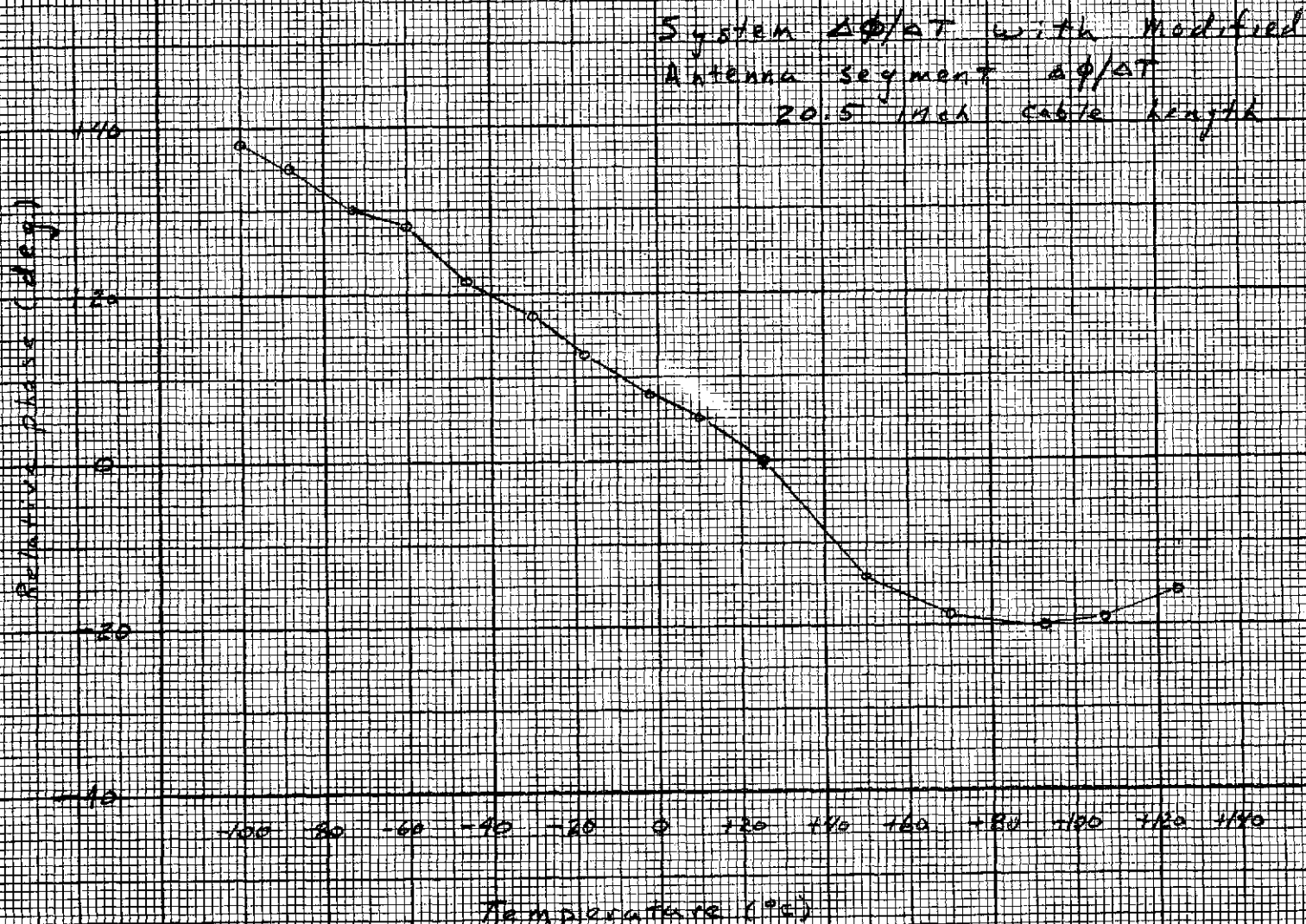


Fig. 11 Extrapolated  $\Delta\phi/\Delta T$  of 17.95-inch Microstrip Transmission Line





18

Fig. 12 System  $\Delta\phi/\Delta T$  with Modified Antenna Segment  $\Delta\phi/\Delta T$  for 20.5-inch coaxial Cable Lenth

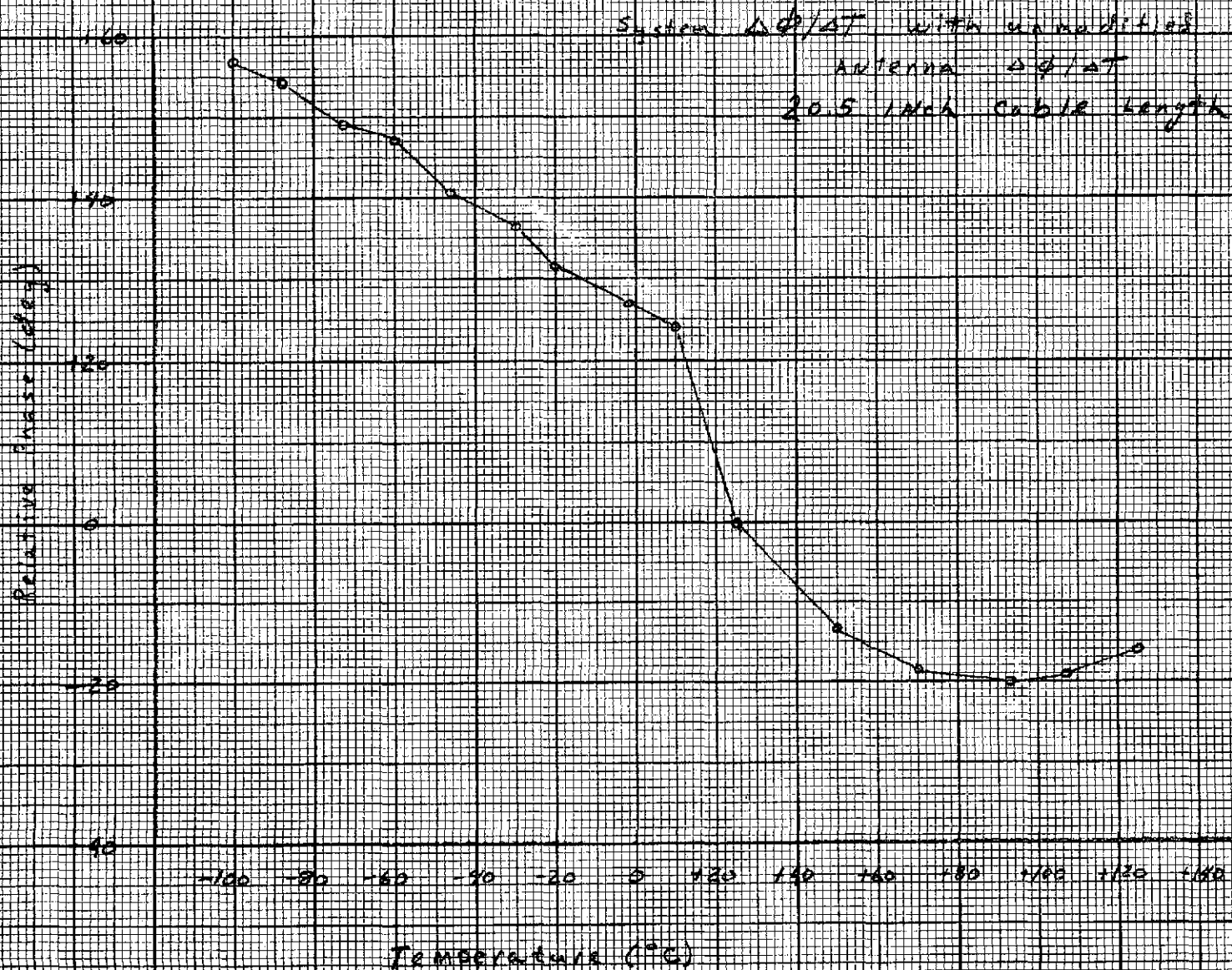


Fig. 13 System  $\Delta\phi/\Delta T$  with Unmodified Antenna Segment  $\Delta\phi/\Delta T$

20

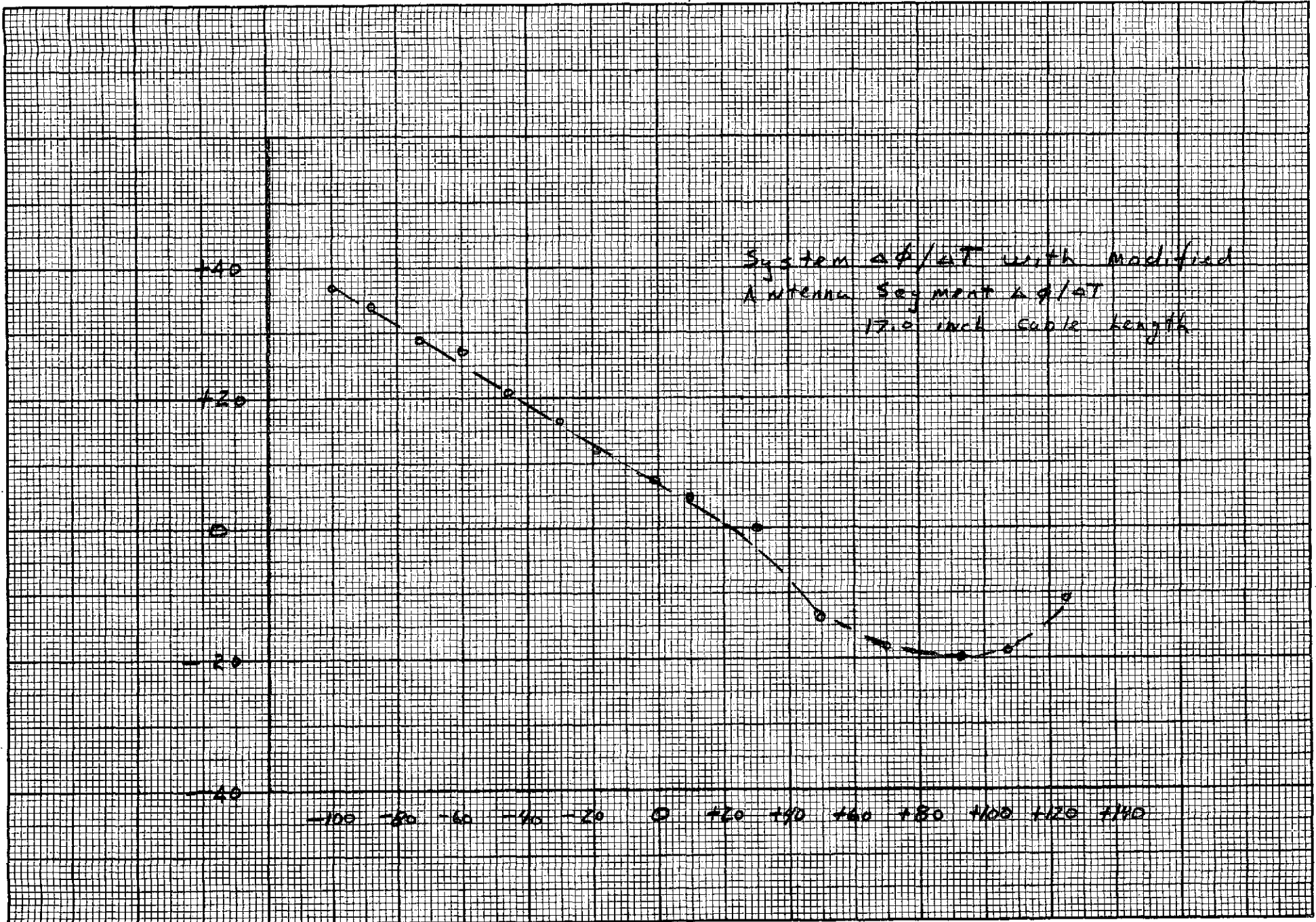


Fig. 14 System  $\Delta\phi/\Delta T$  with Modified Antenna Segment  $\Delta\phi/\Delta T$  for 17-inch Coaxial Cable Length



The test chamber was purged for a longer time prior to testing the 2117 MHz antenna in an effort to minimize the condensation. Again the actual condensation could not be observed, but the average phase change between temperatures for 2117 MHz was  $14.3^\circ \phi$ .

Correspondingly, if we estimate the phase change from  $20^\circ\text{C}$  to  $-10^\circ\text{C}$  on Fig. 12 (no condensation) and Fig. 13 (with condensation) we get  $8.5$  and  $21.0^\circ \phi$  respectively.

It should be noted that during the phase test the cable length between the crystal detector and the antenna and to some extent the crystal itself were cooled. The inclusion of their additional  $\Delta\phi/\Delta T$  due to the feed cable would provide closer agreement between the phase test  $\Delta\phi/\Delta T$  and the  $\Delta\phi/\Delta T$  predicted by analysis.